Influence of Fill Scheme on Oil Sands Tailings Consolidation Modelling in a Geotechnical Centrifuge

by

Taylor Hall

A thesis submitted in partial fulfillment of the requirements for the degree of

Master of Science

in

Geotechnical Engineering

Department of Civil and Environmental Engineering
University of Alberta

Abstract

A series of geotechnical centrifuge modelling experiments were conducted on a kaolinite slurry and treated fluid fine tailings (FFT) material to assess consolidation behaviour. Consolidation modelling for both materials was conducted using both a single and layered fill scheme, and the results were compared. The layered fill scheme was developed to simulate the deposition of tailings more closely at the field scale and how this technique effects results obtained from centrifuge consolidation testing. The centrifuge models were also simulated using a large strain consolidation numerical model and the results were compared. Settlement curves, final void ratio and stress profiles were created for both materials at the end of testing. Both kaolinite and FFT achieved higher settlement in the layered fill tests after similar centrifuge consolidation times, though this value was small (<3%). This discrepancy was attributed to slight variations in initial solids contents for the different tests and variations in the G-level during centrifuge testing. The observed settlement rate was slower in the numerical models compared to the centrifuge tests, but numerical model results were in agreement using an adjusted hydraulic conductivity function for both materials. Significant settlement was observed in the FFT centrifuge models without developing appreciable levels of effective stress.

Preface

This thesis is an original work by Taylor Hall. A portion of this thesis was previously published in: Hall, T., Beier, N. A., Chalaturnyk, R. J. 2018. Influence of Fill Scheme on Slurry Consolidation Modelling in a Geotechnical Centrifuge. Proceedings of the Sixth International Oil Sands Tailings Conference, Edmonton, AB: December 9-12, 2018.

Acknowledgement

I would like to thank the Natural Sciences and Engineering Research Council of Canada (NSERC), Canada's Oil Sands Innovation Alliance (COSIA) and Alberta Innovates – Energy and Environment Solutions for their financial support for this project. I would also like to thank my supervisor Dr. Nicholas Beier for his guidance and insight throughout this research project. Thank you to all the friends and colleagues who have made graduate studies a much more enjoyable and rewarding experience every step of the way. The laboratory component of this research project would not have been possible without the support of Dr. Rick Chalaturnyk, Dr. Gonzalo Zambrano-Narvaez and Yazhao Wang.

Table of Contents

List of Tables

List of Figures

1 Introduction

1.1 Oil sands overview

The mining and extraction of bitumen from Alberta's oil sands produces vast quantities of fluid tailings which require storage in tailings ponds. These fluid tailings contain high percentages of fine particles which require many years to dewater and thus must be contained in large external and in-pit facilities known as tailings ponds. To date, there are over 1200 Mm^3 of oil sands fluid tailings being stored in tailings ponds in Alberta (AER 2019). The end goal for these tailings ponds is reclamation to a natural environment including both terrestrial and aquatic landscapes. Adequate dewatering of these tailings deposits must occur to develop trafficable surfaces which allows for terrestrial reclamation activities to commence (McKenna et al. 2016).

Several technologies have been developed to speed up the natural dewatering process of oil sands tailings. Common technologies used to enhance the dewatering behaviour of oil sands tailings include physical/mechanical processes, natural processes, chemical/biological amendment, mixtures/co-disposal, and permanent in -pit storage options (BGC Engineering Inc. 2010). Some of these tailings dewatering technologies create tailings products which must be adequately studied and characterized to determine their geotechnical properties and long-term dewatering behaviour. The long-term dewatering behaviour of these tailings products can be used to determine tailings storage volumes over the life of the mine and set timelines for reclamation activities.

To predict long-term dewatering behaviour of these tailings products, the effective stress-void ratio and hydraulic conductivity-void ratio relationships are needed. These relationships can be used directly in a finite strain consolidation model to predict settlement. These relationships can be determined using laboratory test methods such as the large strain consolidation (LSC) test (Scott et al. 2008). However, conventional laboratory tests such as the LSC test require weeks or even months to complete. The beam centrifuge provides several advantages over traditional laboratory methods, including reduced testing time (tests can be completed in a matter of hours/days versus weeks/months), and replication of the self-weight stresses in the centrifuge consolidation model (Sorta et al. 2016). Compared to the use of a finite strain consolidation model, the centrifuge modelling technique can be used to directly estimate tailings settlement or can be used to obtain the effective stress-void ratio and hydraulic conductivity-void ratio relationships, as demonstrated by (Sorta et al. 2016, Znidarcic et al. 2011).

Previous centrifuge testing programs which studied oil sands tailings modelled a single fill scheme, in which the centrifuge model of a set starting height is used and allowed to consolidate in the centrifuge (Znidarcic et al. 2011, Sorta et al. 2016, Dunmola et al. 2018). Using the single fill scheme allows researchers to study the consolidation behaviour of a single deposit of tailings in the centrifuge but may not simulate the continuous filling of a tailings pond in the field. Using a fill scheme in which tailings are continually added during testing may provide a closer estimation of the deposition of tailings in the field. A layered modelling procedure was used by (Stone et al. 1994, Antonaki et al. 2017), both with gold mine tailings, but to date the author is not aware of this layered procedure being used with an oil sands tailings material. Developing and testing a layered fill scheme with oil sands tailings may provide additional insight into the consolidation behaviour of these tailings material.

1.2 Scope and Objectives of the Research

The objective of this research was to investigate the use of a new test method for physical modelling of slurry/oil sands tailings consolidation using a geotechnical beam centrifuge. This new test method involves the continuous addition of tailings/slurry material throughout the consolidation process represented by a layered fill scheme. A test procedure using the layered fill scheme will result in different consolidation behaviour compared to the single fill scheme for slurry/oil sands tailings.

A kaolinite slurry and a treated oil sands tailings material were selected for testing. Kaolinite was selected due to its extensive use by other researchers and amount of available data. The kaolinite also serves as a control material when performing identical tests with the oil sands tailings. A flocculated oil sands tailings material was also selected for testing. This material has previously been studied by (Fisseha et al. 2018) and will be used in the centrifuge tests to provide additional insight into the consolidation behaviour of oil sands tailings.

The specific objectives of the research were:

- Develop and test a new method for continuous addition of material during the consolidation process in the geotechnical centrifuge using a layered fill scheme;
- Compare the results obtained using this layered fill scheme with results obtained using a single fill scheme and evaluate the effects of using a layered fill scheme;
- Compare the results obtained from the geotechnical centrifuge tests (single and layered fill schemes) against a numerical model.

1.3 Organization of the thesis

This thesis is organized into six chapters. Chapter 1 provides background on the research project and covers the scope and main objectives of the research. Chapter 2 reviews the relevant literature with respect to consolidation modelling using a geotechnical centrifuge; a review of oil sands tailings literature is also included. Chapter 3 outlines the materials and methods that were used for the laboratory testing component, as well as the numerical modelling methodology. Chapter 4 presents the experimental results. Chapter 5 provides a discussion of the experimental results. Chapter 6 summarizes the conclusions of the research program and suggestions for future work.

2 Centrifuge Modelling and Literature Review

2.1 General

This chapter includes an introduction, description and literature review of the centrifuge modelling principle and its application to geotechnical engineering problems, including self-weight consolidation modelling. A review of oil sands literature is also provided to summarize oil sands mining/extraction, geology/mineralogy, oil sands tailings production, and the consolidation behaviour of oil sands fine tailings.

2.2 Centrifuge Modelling Principle

2.2.1 Centrifuge Overview

A centrifuge is a device which puts an object into rotation about a fixed axis, creating a force perpendicular to the axis of rotation. In the field of geotechnical engineering, centrifuges can be used to simulate high acceleration stress fields beyond that created by Earth's gravity. Because gravity is often the primary driving force in geotechnical engineering problems, centrifuge modelling can be used to create small-scale models of geotechnical structures, such as slopes, retaining structures, underground excavations, self-weight consolidation and groundwater contaminant migration. The mechanical properties of soil are dependent on both stress level and stress history, therefore any physical modelling should preserve the similitude of stress profiles between the prototype (field) and model scale. Geotechnical centrifuge modelling allows researchers to replicate the prototype stress conditions in small-scale, laboratory controlled physical models.

The self-weight stresses experienced by a soil deposit are a product of the soil unit weight and the thickness of the soil deposit. To produce an equal stress level between a prototype and a small-scale

model, the unit weight of the soil in the model must be increased. At the prototype scale, soil unit weight is a function of the soil density and Earth's gravity (g) (Figure 1). In the geotechnical centrifuge, the primary driving force is centrifugal acceleration generated by rotating around the centrifuge axis. Therefore, soil unit weight in the centrifuge is a function of centrifugal acceleration and soil density (Figure 2). At any height, h_p, in the prototype scale, the soil experiences a stress equal to σ_p. At the model scale, the soil experiences the same stress ($\sigma_p = \sigma_m$), however, the stress occurs at a height of h_m, where $h_p/h_m=N$, where N is the acceleration level in the centrifuge relative to Earth's gravity. This is the fundamental scaling law of centrifuge modelling (Taylor 1995). From this relationship, it is shown how centrifuge modelling replicates the self-weight stress of a prototype at the model scale.

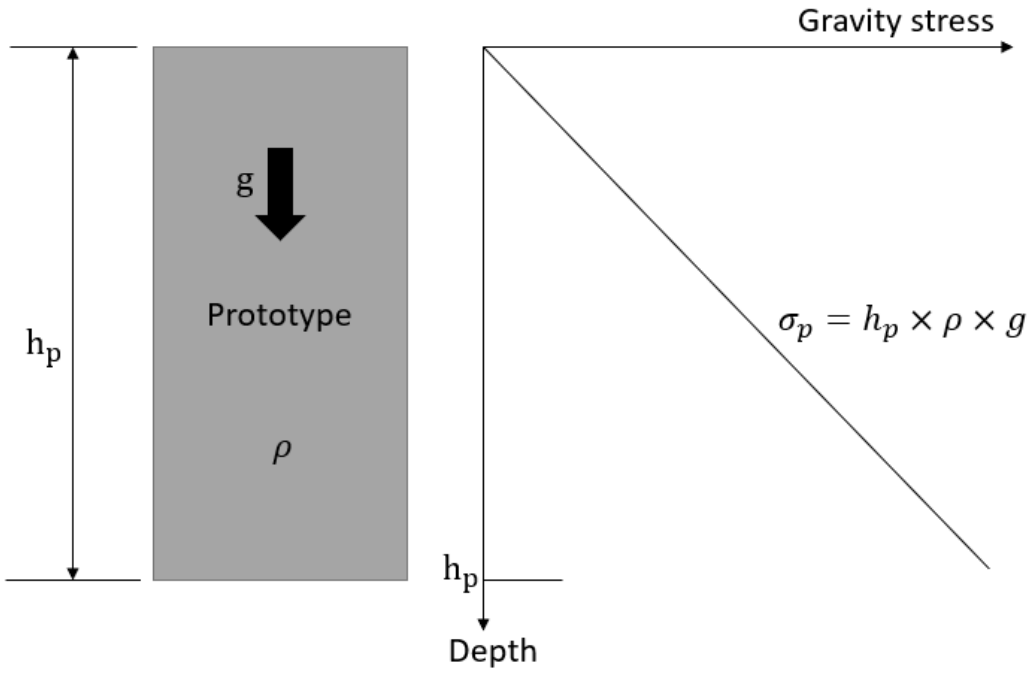

Figure 1 - Stress Distribution in Prototype, Modified from Taylor (1995)

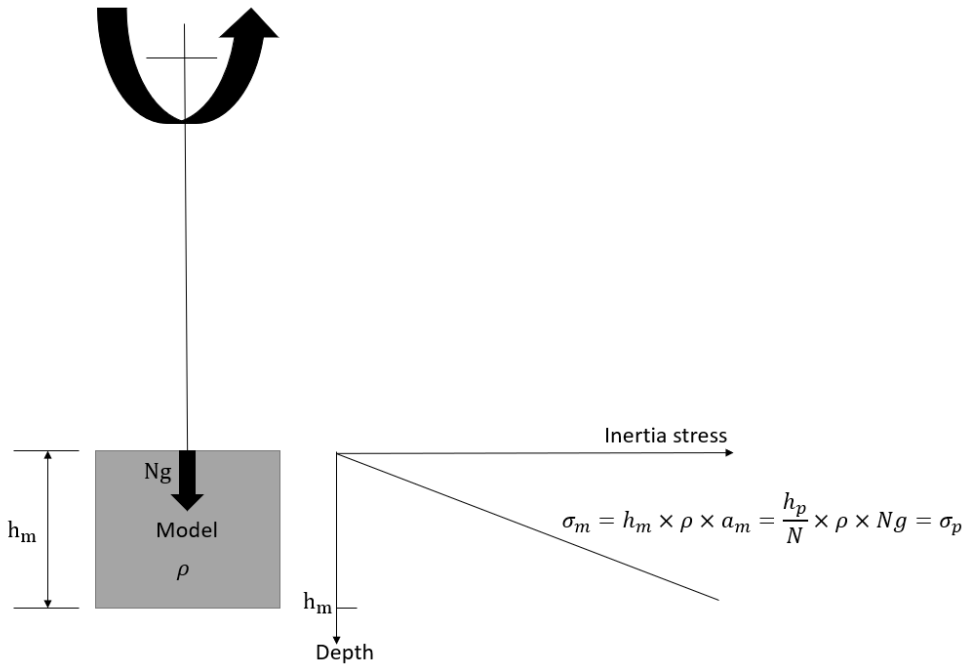

Figure 2 - Stress Distribution in Centrifuge Model, Modified from Taylor (1995)

Acceleration due to Earth's gravity is constant, therefore at the prototype scale the stress distribution at the prototype scale is a linear relationship increasing with depth (Figure 3). However, at the model scale in the centrifuge, acceleration is calculated as $\omega^2 r$, where ω is the rotational speed of the centrifuge and r is the radius to any point in the soil (Taylor 1995). The stress distribution with depth at both the prototype and model scale is shown in Figure 3. Due to the non-linear stress distribution at the model scale, there are points of both over-stress and under-stress in centrifuge models relative to the prototype stress distribution (Figure 3). However, this error can be accounted for by equating the prototype and centrifuge model stress at the point where the stress profiles are equal. This point is given as (Taylor 1995):

$$R_e = R_t + \frac{h_m}{3} \quad [1]$$

Therefore, the effective centrifuge radius should be measured from the centre of the centrifuge axis to one third the model depth (Taylor 1995). For most geotechnical centrifuges (including the one used in

this study), the model height is less than 20% of the centrifuge radius, therefore the maximum error is less than 3% between the prototype and model stress profiles (Taylor 1995).

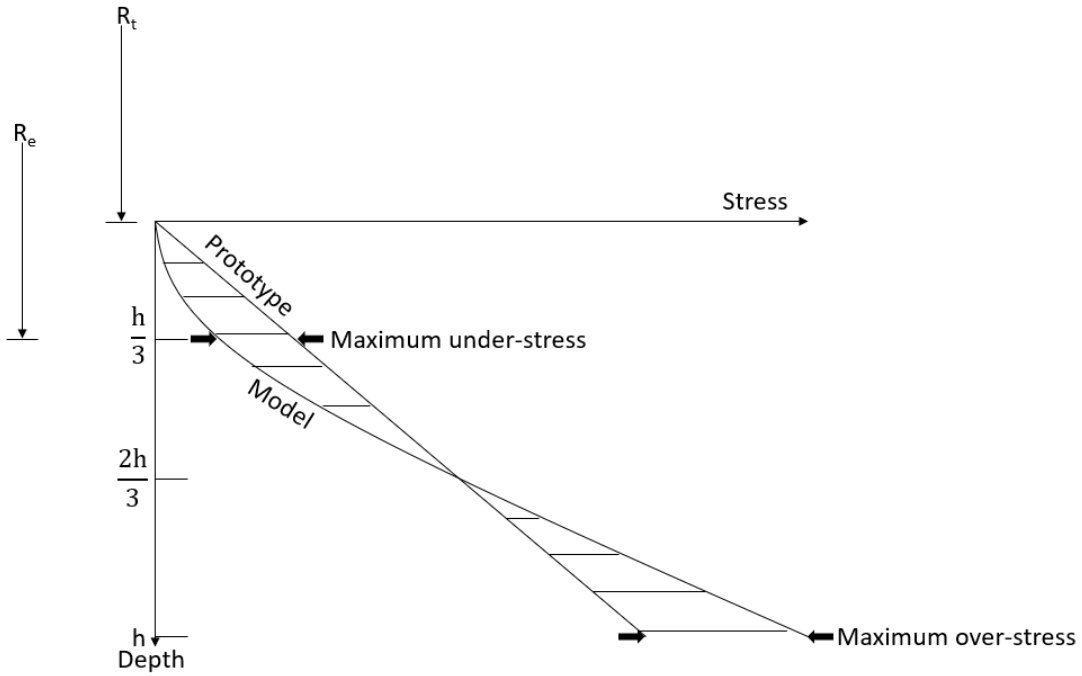

Figure 3 - Stress Distribution with Depth in Prototype and Centrifuge Model, Modified from Taylor (1995)

2.2.2 Scaling Laws

The geotechnical centrifuge can be used for modelling a variety of geotechnical problems. As demonstrated in the last section, the geotechnical centrifuge maintains stress profiles between the model and prototype. Additional physical phenomenon can also be scaled in the centrifuge, including consolidation. The consolidation time between model and prototype is scaled as follows (Roscoe 1968, Cargill and Ko 1983, Eckert et al. 1996):

$$t_m = \frac{t_p}{N^2} \quad [2]$$

Where t_m is elapsed time in the centrifuge model, t_p is elapsed time at the prototype scale at the same degree of consolidation, and N is the acceleration level in the centrifuge. As an example, a 100-G spin for 0.88 h would model one year of consolidation at the prototype scale. Scaling laws for other physical properties are shown below in Table 1.

Table 1 - Centrifuge Scaling Laws, Modified from (Sorta 2015)

Property	**Model**	**Prototype**
Length	1	N
Acceleration	N	1
Density	1	1
Time (consolidation)	1	N^2
Time (creep)	1	1
Settlement	1	N
Strain	1	1
Strain rate	N^2	1
Pressure	1	1
Hydraulic gradient	1	1
Flow velocity	N	1
Hydraulic conductivity	N	1

2.2.3 Modelling of Models

The modelling of models technique can be used in centrifuge tests to determine the validity of a centrifuge model (Ko, 1988). This experimental technique involves running three different centrifuge models of varying heights and acceleration (G-levels), but all representing the same prototype. This technique is demonstrated below in Figure 4. The centrifuge models A1, A2, and A3 all show models of different heights and different G-levels, but all represent the same prototype of 1 m height. Results from the three centrifuge models can be compared to determine the stress and scale effects on the centrifuge model.

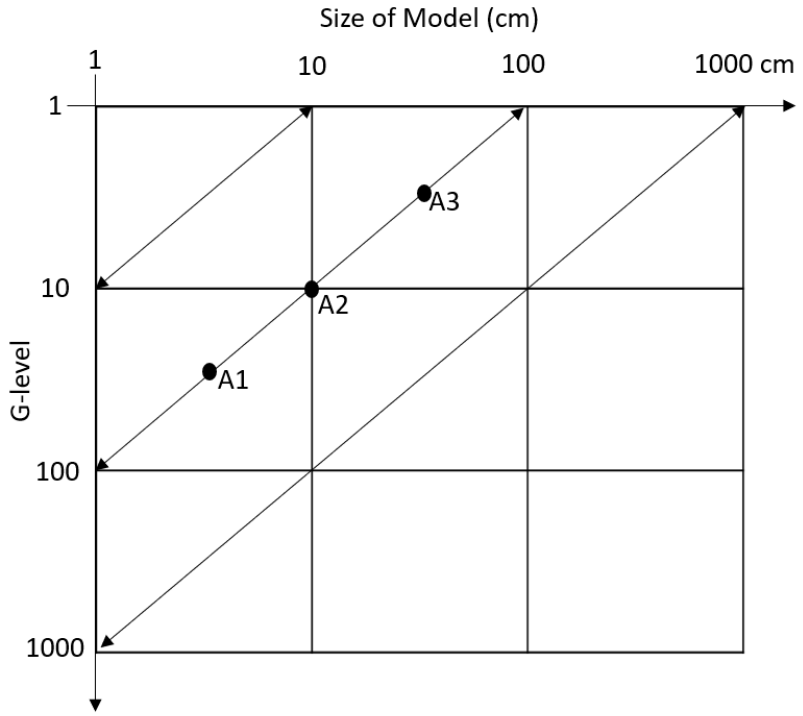

Figure 4 - Modelling of Models Principle, modified from Ko (1988)

2.3 Centrifuge Literature Review

This section of the literature presents and summarizes the use of geotechnical centrifuge technology in experimental programs.

Cargill and Ko (1983) derived theoretical scaling relationships between a centrifuge model and prototype for water flow through a soil embankment. The researchers used a 1.36m radius beam centrifuge at the University of Colorado to model transient water flow through a soil embankment and verify theoretically derived scaling laws. The model soil embankments were instrumented with miniature pore pressure transducers and monitored on a closed-circuit TV during testing. Four different soil samples were tested, consisting mainly of reconstituted mixtures of sand and silts with varying grain size distributions. Nine tests were conducted on each different soil embankment. Pore pressure transducers were placed at the 1-in, 3-in, and 5-in levels in the model embankments and tests were ran at 25g, 37.5g and 50g at each pore pressure transducer arrangement. Tailwater levels were maintained throughout testing via an external drain. Headwater levels were varied during testing via an external drain and external water supply. Five different headwater levels were used for each soil type and g-level to generate equipotential distributions in the model embankments. The researchers concluded that the

centrifuge modelling technique was valid and practical for modelling transient flow phenomenon and results were consistent with theoretical predictions.

Townsend et al. (1986) used a 1m radius beam geotechnical centrifuge at the University of Florida to study the consolidation behaviour of waste clays from phosphate production and evaluate different reclamation schemes. The researchers chose to use the geotechnical centrifuge in favour of traditional methods such as bench tests with graduated cylinders to reduce testing time and maintain stress levels between centrifuge models and prototypes. The researchers conducted centrifuge tests on models from 8cm to 12cm in height at g-levels of 60g to 80g to model the consolidation of 4.8 m to 9.6m waste ponds. Test materials varied in solids content from 14% to 20%. The researchers used the modelling of models technique to derive time scaling factors, which was found to be between 1.6 and 2.0 depending on the initial solids content of the material tested. Centrifuge modelling was shown to be a viable technique for examining disposal schemes of phosphate waste clays.

Takada and Mikasa (1986) used a 1.75m radius beam centrifuge at Osaka City University to determine the consolidation parameters of four different soft clay samples. The geotechnical centrifuge was chosen for its ability to maintain stress profiles between models and prototype, reduce total testing time, and avoid the complexities associated with other testing methods such as the seepage consolidation test and the constant rate consolidation test. Centrifuge tests were conducted at 100g and 150g for different clay samples. The researchers were able to successfully determine the volume compressibility, permeability, and coefficient of consolidation of the soft clay samples using the centrifuge consolidation test. The centrifuge consolidation test provided test results with accuracies similar to those obtained from oedometer tests, however the centrifuge tests can be completed on samples with much higher water contents.

Stone et al. (1994) used a 1.8m radius beam centrifuge at the University of Western Australia to study the short and long-term consolidation behaviour of gold mine tailings. The centrifuge tests were designed to replicate the staged filling of an existing tailings impoundment with available field data. The centrifuge model was constructed by successively adding layers of material (with the centrifuge stationary) and allowing individual layers to consolidate. The thickness of each added layer was chosen to replicate the available field measurements. Once the model had reached its final height, it was instrumented with additional pore pressure sensors and placed back on the centrifuge platform to assess the long-term consolidation behaviour. Numerical modelling was also completed on the tailings

impoundment to provide additional data for comparison. The researchers noted good agreement between field and centrifuge model data, as well as with numerical model results.

Singh and Gupta (2000) used a small beam centrifuge (radius 200mm) to determine the hydraulic conductivity of a soil sample. The researchers prepared the soil to ten different compaction levels and evaluated the use of a centrifuge to determine the hydraulic conductivity of each sample. Soil samples were 30mm thick and the centrifuge tests were designed to simulate a falling head test. The hydraulic conductivity values obtained from the centrifuge tests were compared to those obtained from conventional falling-head tests, oedometer falling-head tests and consolidation tests. The researchers concluded that the centrifuge hydraulic conductivity test provided good results compared to the traditional methods and testing for hydraulic conductivity using the centrifuge technique can be completed in a shorter period compared to traditional methods.

Fox et al. (2005) developed a numerical model for one-dimensional large strain consolidation in a geotechnical centrifuge. The numerical model was built to simulate the varying acceleration with depth in the geotechnical centrifuge. The numerical model was validated by conducting a series of centrifuge consolidation tests on samples of Singapore marine clays. Numerical simulations were run with varying model heights, effective radius, acceleration levels and initial height to effective radius ratios to determine the effect of the non-uniform acceleration experienced by a centrifuge model. The settlement-time curves from the centrifuge tests were compared to those obtained from the numerical model, and it was found that the computed consolidation error was controlled by the initial height to centrifuge radius ratio, though this value was small at ratios of 0.2 or less.

Znidarcic et al. (2011) used a geotechnical centrifuge to study consolidation behaviour of oil sands mature fine tailings (MFT). In this test, an 82mm MFT column was accelerated to 45g and allowed to consolidate. Consolidation of the MFT column was monitored in-flight by a camera. The settlement-time curves and final void ratio profiles were generated for the MFT model and compared to results obtained from a numerical model. The researchers used the seepage induced consolidation test to determine the input parameters for the numerical model (void ratio-effective stress and hydraulic conductivity-void ratio curves). The centrifuge test results were in good agreement with the numerical model results and indicated that oil sands MFT have similar consolidation behaviour to other slurry mixtures. The researchers note that field consolidation of MFT does not occur as expected compared to controlled laboratory conditions, and this may be attributed to the variations in the hydraulic gradient between the field and the laboratory conditions.

Sorta et al. (2012) used a 5.5m radius beam centrifuge to examine the effect of thixotropy and segregation on centrifuge consolidation modelling. Settling column tests and centrifuge tests were used to establish the segregation boundaries of various oil sands tailings mixtures on a ternary diagram. In the settling column tests, tailings mixtures were prepared and allowed to settle in a column of 32cm for one month. Tailings mixtures were prepared to different solids and fines contents to establish the segregation boundaries. In the centrifuge tests, a series of PVC cylinders were filled with tailings mixtures of varying solids and fines contents and allowed to settle in the centrifuge at 60 or 100g, depending on the test. The segregation boundaries were established from the centrifuge tests by sampling the material at different heights and plotting the results on a ternary diagram. Results from these tests show that high acceleration levels in the geotechnical centrifuge enhance segregation of oil sands tailings mixtures. The authors indicate that this enhanced segregation observed in the centrifuge tests is a result of the high acceleration levels increasing the weight of individual coarse grains (sand) but leaving the fines carrying capacity unchanged. Increased segregation in the centrifuge tests limits the material compositions that can be used and the consolidation parameters that can be derived from centrifuge modelling. It is noted that segregation in the centrifuge can be reduced by allowing test materials to sit for 24 hours prior to centrifuge testing. The authors also conducted a series of tests on oil sands tailings mixtures of various initial compositions to determine their thixotropic strength gain with time. Results from these tests indicated that oil sands tailings are highly thixotropic materials, and thixotropic strength gain is primarily a time-dependant and not gravity-dependant process. The authors indicate that centrifuge tests do not properly account for strength gains due to thixotropy and makes it difficult to extrapolate centrifuge test results at the prototype scale.

Reid and Fourie (2012) developed a modified desktop centrifuge that can be used to determine the consolidation parameters for a variety of soils. The authors used a modified Clements Orbital 420 desktop centrifuge and outfitted the device with digital speed (RPM) control, replaced the test tube holders with polycarbonate columns to hold samples, and installed piezometers and data transmitters at the bottom of the sample columns. Kaolin clay samples were placed into the desktop centrifuge device and allowed to consolidate between 1000 and 1400 RPM. After testing, the samples were excavated and the moisture content (void ratio) profiles with depth were determined. Total stress, pore water pressure and effective stress profiles with depth were also established. These results were combined to generate a void ratio-effective stress curve for the samples. Void ratio-effective stress curves generated from these tests were found to be in good agreement with other literature results.

Kayabali and Ozdemir (2012) used a miniature centrifuge to assess its practicality for 1-D consolidation testing compared to traditional oedometer tests. The centrifuge used in these tests had a radius of 0.35m and was capable of spinning samples up to 3000 RPM. In total, 32 tests were conducted using the centrifuge apparatus and oedometer. The researchers note that it was not possible to directly match centrifuge and oedometer data pairs based on applied effective stress, so data points were matched based on total vertical settlement of the samples. Good correlation was found between applied effective stress in the oedometer and applied centrifugal force in the centrifuge when both samples achieved the desired amount of settlement. This correlation was used to convert applied centrifugal force to effective stress, thus allowing the generation of vertical strain-effective stress plots for both oedometer and centrifuge tests. Results from these tests indicate good agreement between oedometer and centrifuge 1-D consolidation tests. The authors were also able to derive the recompression index, compression index, and the preconsolidation pressure from the centrifuge tests with good accuracy.

Sorta et al. (2016) used a 2m geotechnical beam centrifuge at the University of Alberta to physically model oil sands tailings consolidation. A series of tests were conducted on kaolinite slurry and oil sands tailings of different initial compositions (source location and solids contents). A series of tests were run to verify the repeatability and verify centrifuge scaling laws. The verification tests included modelling of models, repeating tests conducted at other centrifuge facilities, and comparison of test results with those obtained from 1g tests. Repeatability and verification of centrifuge scaling laws was successful. Centrifuge tests were conducted on oil sands tailings mixture and kaolin clay slurry between 40 and 100g, and initial sample heights between 10 and 24cm. Interface settlement was monitored in-flight with scales attached to the inside wall of the test cells via an externally mounted HD camera. Laser displacement sensor was also used to monitor interface settlement in-flight. Pore pressure transducers were attached to centrifuge test cells and pore pressure data was obtained in-flight. Solids content was also monitored in-flight via time domain reflectometry instruments. Settlement curves were generated from the centrifuge tests. Void ratio-effective stress and permeability-void ratio curves were also generated from the centrifuge tests and used as inputs for large strain numerical models. Numerical models were also run based on inputs from large strain consolidation (LSC tests, and the results were compared. Void ratio-effective stress curves generated from centrifuge and LSCT tests showed good agreement, and ultimate settlement values from the numerical models was in close agreement. At different elapsed times, numerical model predictions for settlement based on LSCT inputs were lower than those from centrifuge. This is due to the permeability-void ratio relationships being higher in the centrifuge tests as compared to LSCT. The authors note, however, that increasing the hydraulic

conductivity of the LSCT inputs by less than one order of magnitude resulted in good agreement between the numerical model and centrifuge results.

Antonaki et al. (2017) used a geotechnical centrifuge to evaluate the consolidation and dynamic response of a layered gold mine tailings deposit. The centrifuge models were instrumented with pore pressure sensors, settlement gauges, bender elements and LVDTs. The centrifuge models were constructed in 6 layers, with consolidation of each layer allowed to occur at 20g before a new layer was added. The consolidation of individual layers allowed the authors to install embedded sensors into the model, as the consolidated material gained strength after consolidation. Centrifuge tests were conducted at 80g once the models were fully constructed. In the consolidation tests, significant settlement of the model occurred during loading of the individual layers at 20g. Centrifuge models were then subjected to a moderately strong harmonic motion to evaluate their response to dynamic loading. Pore pressures, lateral displacements and shear wave velocities were measured during the dynamic loading phase. The authors observed liquefaction of the mine tailings during the dynamic loading phase based on the pore pressure responses, and a mild slope that was excavated in the centrifuge model was flattened after the dynamic loading test. Results from these tests indicate that a layered model can be used for consolidation modelling in the centrifuge.

Dunmola et al. (2018) used a 2m beam centrifuge at the University of Alberta to compare physical model results from centrifuge tests to full-scale settling columns. A series of centrifuge tests were also conducted to validate centrifuge scaling laws for a fluid fine tailings (FFT) mixture. Tests were conducted at 80, 100, and 120g with initial model heights of 15, 12 and 10cm, respectively, for modelling of models tests for the FFT material. Results from the modelling of models test indicate that centrifuge scaling laws are valid for the test material. A series of 6 full-scale columns were constructed and monitored to evaluate the long-term performance of the FFT material and compare different tailings management technologies. The columns are 11m in height and 3m wide, with different boundary conditions used to assess different tailings management technologies. Columns were instrumented with settlement monitors and vibrating wire piezometers for pore pressure measurements. Results from the settling column tests were compared to results obtained from the centrifuge. Deformation and pore pressure responses in the column and centrifuge tests were in good agreement and demonstrate the validity of the geotechnical centrifuge for predicting the long-term performance of this particular oil sands tailings material.

As demonstrated by this literature review, significant research has been conducted in the area of centrifuge modelling and its application to geotechnical problems. Research has been conducted to verify the validity of centrifuge modelling techniques, study geotechnical problems such as seepage and one-dimensional consolidation, and has been used to study large strain consolidation (including mine waste deposition). Although formal studies have been conducted using the centrifuge modelling technique for mine waste problems, research in this field is still needed. The work presented in this thesis will study the consolidation behaviour of a treated oil sands tailings product and will investigate the consolidation behaviour of this material while attempting to more closely replicate the deposition of tailings at the field scale.

2.4 Oil Sands Literature Review

2.4.1 Introduction

The oil sands of northern Alberta contain the third largest proven oil reserves in the world and cover an area approximately 142,200km^2. This total area is divided into three main geographic area that include the Athabasca, Cold Lake and Peace River oil sands deposits (Government of Alberta 2018). In total, the oil sands contain 177 billion barrels (28 billion m^3) of proven bitumen reserves (AER 2018). Approximately 3.4% of the total oil sands area (4,800km^2) contain shallow oil sands deposits (<75m depth) that can be extracted with surface mining techniques; the remaining deposits can be accessed with in-situ extraction techniques (Government of Alberta 2018). Surface mining of oil sands deposits takes place exclusively in the Athabasca oil sands region near Fort McMurray, Alberta.

2.4.2 Geology and Mineralogy

The bitumen deposits in the Athabasca oil sands are contained primarily within the Lower Cretaceous McMurray-Wabasca geologic formation, originally deposited approximately 110 million years ago (Mossop 1980). This formation varies up to 150m in thickness and contains primarily uncemented sands and shales underlain by Devonian limestone (Flach 1984). The Athabasca oil sand consists primarily of quartz grains (95%), feldspar grains (2 to 3%), mice flakes and clay minerals (2 to 3%), and other trace minerals (Mossop 1980). Clay bands are present in the oil sands, varying from 1 to 15cm in thickness and are made up primarily of kaolinite (40 to 70% by weight), illite (28-45% by weight) and montmorillonite (1-15% by weight) (Chalaturnyk et al. 2002). Bitumen content in the Athabasca oil sands ranges from 0 to 19% by weight (average 12%), with an average water content between 3 to 6% by weight (Chalaturnyk et al. 2002).

2.4.3 Oil Sands Mining and Extraction

Oil sands mining begins by first removing overlying muskeg, vegetation and tree cover. Suitable soil material that is removed during overburden stripping is stockpiled and used later for reclamation activities. Rock, clay and sand overburden materials are then removed to expose the oil sands deposits below (NEB 2000). Oil sands are excavated at the mine face with large shovels and transported to crushers by haul trucks (NEB 2000). At this stage, the crushed oil sands are mixed with hot water and caustic soda (sodium hydroxide, NaOH) to condition it for bitumen separation (NEB 2000). This process is based on the Clark Hot Water Extraction Process (Klark and Pasternack 1949). Following this initial conditioning, the oil sands are transported via pipeline to primary separation vessels where the coalescence of bitumen particles leads to flotation of the bitumen; this bitumen froth is then skimmed off for further processing (Chalaturnyk et al. 2002). The centre part of the primary extraction stream (middlings) is pumped back into the main feed and to scavenger cells for further processing to capture additional bitumen (Chalaturnyk et al. 2002). Coarse materials that settle to the bottom of the primary separation vessels and scavenger cells are discarded to the tailings stream (Chalaturnyk et al. 2002). The extraction process is able to recover approximately 90% of the bitumen, and recovery rates are improving with technological advancements (Chalaturnyk et al. 2002); (NEB 2000).

2.4.4 Tailings Production

The extraction of bitumen from oil sands results in three primary tailings streams: coarse tailings, fine tailings, and froth treatment tailings (Kasperski and Mikula 2011). The coarse tailings stream is produced from the cyclone underflow (CUF) materials during the primary extraction stages; these coarse materials are primarily sands (>44µm diameter) (Kasperski and Mikula 2011, Jeeravipoolvarn 2010). Fine tailings, produced from cyclone overflow (COF) consist mainly of fine clays and silts (<44µm diameter) (Kasperski and Mikula 2011, Jeeravipoolvarn 2010). The third tailings stream, froth treatment tailings, result from the mixing of bitumen and solvents such as naptha that aid in recovery of the bitumen (Kasperski and Mikula 2011). Froth treatment tailings are a mixture of water, sand, silt, clay, residual bitumen and solvent (Kasperski and Mikula 2011).

Tailings materials are discharged to large containment areas known as tailings ponds, where the coarse fraction quickly settles out and can be used as construction material for dykes and beaches (Jeeravipoolvarn 2010). The coarse tailings stream can also be used in the production of engineered tailings such as composite tailings (CT) and non-segregating tailings (NST) (Nik 2013). The fines fraction of tailings does not settle out during deposition, but instead accumulates in the center of the tailings

ponds and forms what is know as fluid fine tailings (Jeeravipoolvarn 2010). These fluid fine tailings begin to settle in the tailings ponds, and form mature fine tailings (MFT) at a solids content of 30% (Jeeravipoolvarn 2010). The slow dewatering behaviour of MFT has resulted in the accumulation of large quantities of tailings requiring long-term storage in tailings ponds (Kabwe et al. 2014). To date, there are over 1.1 billion m^3 of accumulated fluid fine tailings in oil sands tailings ponds (AER 2016).

2.4.5 Tailings Reduction

There are several technologies that have been developed to reduce the volume of stored tailings in the oil sands industry. The primary goal of tailings reduction technologies is the reduction of stored water within the tailings matrix, which leads to tailings deposits with increased strength and limited compressibility (Sobkowicz and Morgenstern 2009). The improved geotechnical characteristics of tailings by dewatering would then assist in the goal of reclaiming tailings deposits to a natural landscape. There are several tailings reduction technologies currently in use in the oil sands, as described below.

Composite tailings (CT) are a mixture of MFT and COF, and this mixture is chemically treated with gypsum to produce a non-segregating material with a sand to fine ratio (SFR) between 3 and 5 (Nik 2013). Compared to untreated tailings, composite tailings settle, consolidate and develop effective stress quickly (Nik 2013). A similar product, non-segregating tailings, are produced by mixing thickened tailings (described below) with sand from COF tailings.

Thickened tailings (TT) are produced from COF material that is then mixed with a flocculant and dewatered. The final product has a solids content of ~50% (Nik 2013). A similar product, known as in-line thickened tailings (ILTT), is also produced from COF material but is mixed in-line with a flocculating agent and deposited directly into a tailings pond (Jeeravipoolvarn 2010).

Thin lift drying can be used with different tailings products, and refers to the deposition of tailings in thin lifts which allows solid particle to settle, released water to drain, and exposed material to air dry prior to the addition of a new layer of material being added (Nik 2013). Thin lift drying technology is currently utilized by two oil sands operators (COSIA 2018).

Fluid fine tailings treated with a flocculant and further dewatered by using solid-bowl scroll centrifuges are referred to as centrifuge tailings. Centrifuge tailings have a final solids content of ~55% after processing and are deposited in thin lifts or deep deposits where they continue to release water. Centrifuge cake that is deposited in thin lifts and exposed to one freeze-thaw cycle during the winter will attain a peak shear strength of 5-10 kPa before an additional lift of material is placed (OSTC 2012).

2.4.6 Consolidation Behaviour of Oil Sands Fine Tailings

Oil sands tailings are primarily deposited as slurries and undergo significant volume (void ratio) changes during consolidation. Because of these large void ratio changes, Terzaghi's classical theory of one-dimensional consolidation is not appropriate when trying to quantify the consolidation of oil sands tailings. Instead, large strain theory, originally described by (Gibson et al. 1967), is used. Gibson's large strain theory accounts for changes in void ratio and permeability of slurry material as it consolidates and allows more accurate predictions of consolidation behaviour (Gibson et al. 1967). More specifically, the effective stress-void ratio and hydraulic conductivity-void ratio relationships can be used as inputs for finite strain consolidation models to predict the amount and rate of settlement (Scott et al. 2008).

The large strain consolidation test can be used to directly obtain both void ratio-effective stress and hydraulic conductivity-void ratio relationships (Scott et al. 2008). The large strain consolidation test involves step-loading of a slurry sample with an applied stress and recording the void ratio-effective stress values at each increment (Scott et al. 2008). At each interval, a constant head upwards flowing permeability test is performed to obtain the hydraulic conductivity-void ratio relationship (Scott et al. 2008).

Void ratio-effective stress and hydraulic conductivity-void ratio relationships can also be obtained directly from geotechnical centrifuge tests. The test method used to derive large strain consolidation relationships is described in (Sorta et al. 2016). Time domain reflectometry (TDR) was used to monitor solids content with depth in the centrifuge samples during flight and used to generate the hydraulic conductivity-void ratio relationships (Sorta et al. 2016). Effective stress data was obtained from pore pressure sensors and were also monitored in-flight. Centrifuge derivation of the void-ratio effective stress and hydraulic conductivity-void ratio relationships can be advantageous compared to the large strain consolidation test, as the centrifuge method can be completed in a relatively short time, as compared to the large strain consolidation method which may take weeks or even months to complete (Sorta et al. 2016). Void ratio-effective stress and hydraulic conductivity-void ratio relationships were compiled by (Jeeravipoolvarn 2005) and are shown in Figure 5 and Figure 6.

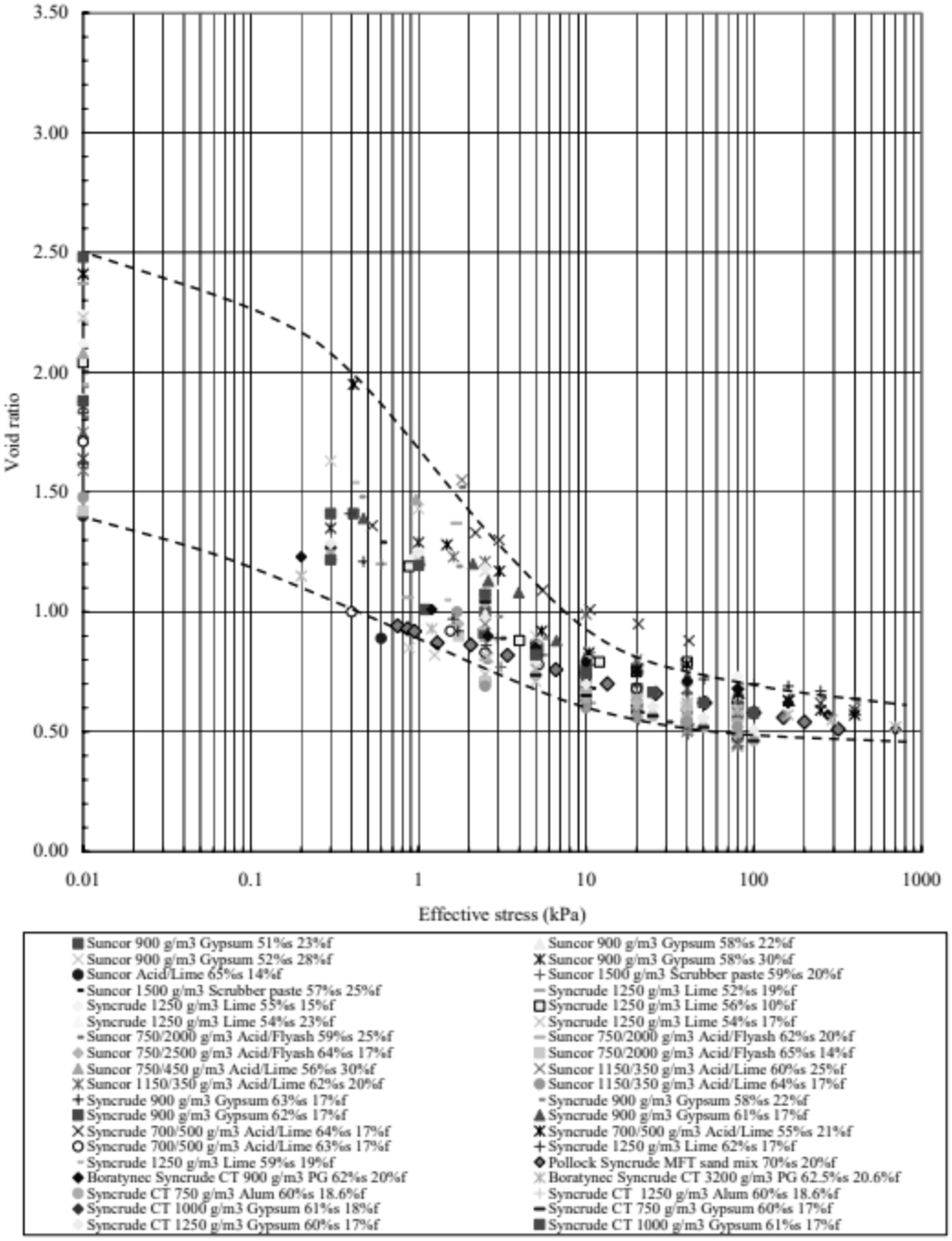

Figure 5 - Void Ratio-Effective Stress Relationships for a Variety of Oil Sands Tailings Materials (Jeeravipoolvarn 2005)

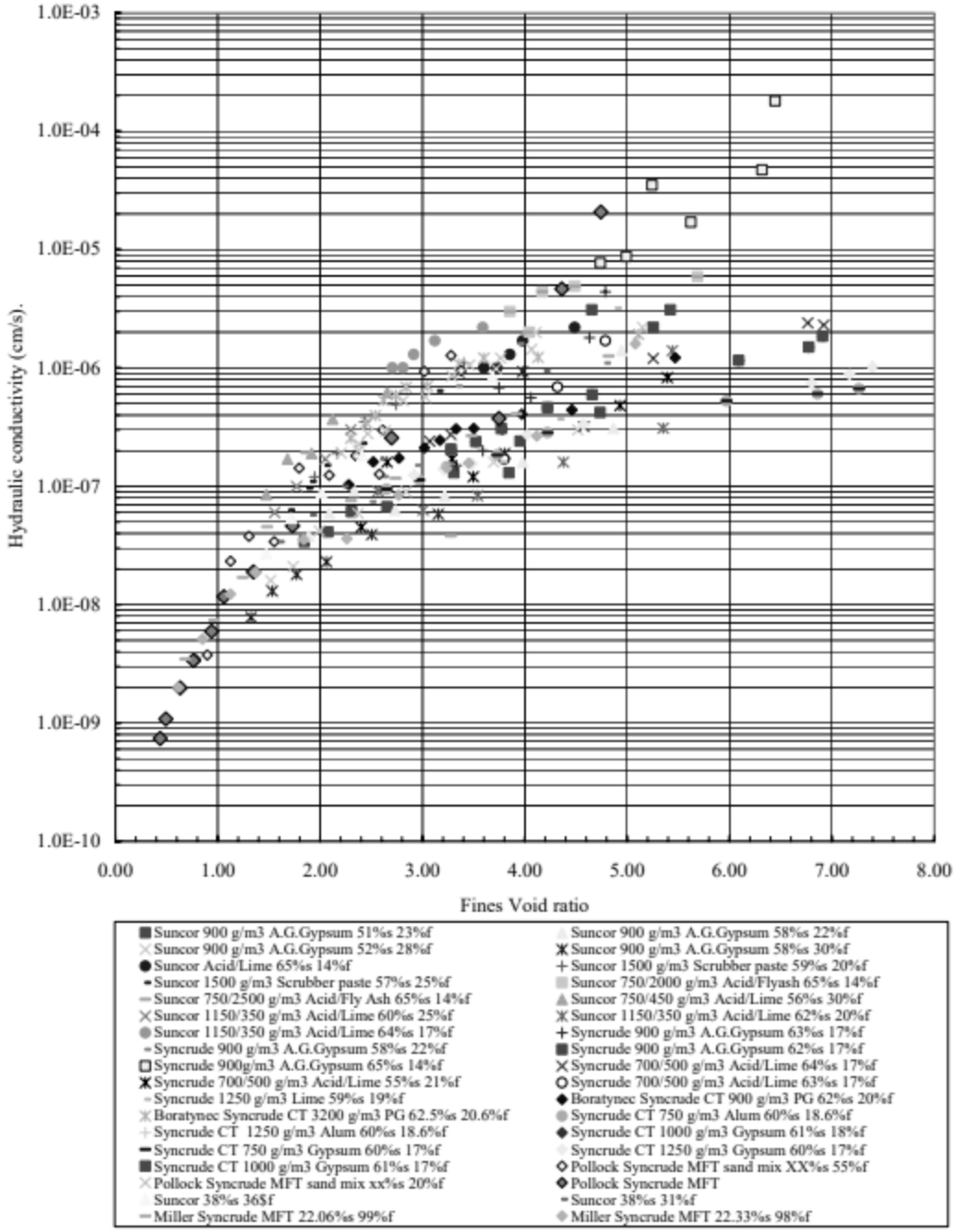

Figure 6 - Hydraulic Conductivity-Void Ratio Relationship for Various Oil Sands Tailings Materials (Jeeravipoolvarn 2005)

3 Test Materials and Procedures

A kaolinite slurry and oil sands tailings were used for the tests in this study. A detailed description and characterization of each material is provided in the following sections. The centrifuge test procedures and test conditions are also outlined.

3.1 Test Materials

3.1.1 Kaolinite Slurry

The kaolinite slurry was prepared by mixing Edgar Plastic Kaolin (EPK) clay with distilled water with a mud mixer in a 20L pail. The slurry was mixed thoroughly, and no unmixed material was observed after preparing the material. No other additives were included in this mixture. The geotechnical properties of the EPK clay are shown in Table 2.

3.1.2 Oil Sands Fluid Fine Tailings

The oil sands tailings used in this study were fluid fine tailings (FFT) provided by the Oil Sands Tailings Research Facility (OSTRF) located in Devon, Alberta, Canada, originally sourced from a mine operator in northern Alberta. The material arrived untreated in 20L pails at a solids content of 52%. The geotechnical properties of the FFT are shown below in Table 2. To determine the full grain size distribution, four samples of material were obtained from the pails and hydrometer tests were completed (ASTM International 2017). These results are shown in Figure 7. An x-ray diffraction (XRD) analysis was completed on a sample of the tailings materials to determine the full mineralogy. These results are presented in Figure 8.

Table 2 - Geotechnical Properties of Kaolinite Clay and Oil Sands Fluid Fine Tailings

Material Description	**Bitumen Content (%)**	**Liquid Limit (%)**	**Plastic Limit (%)**	**Fines (<45µm) (%)**	**Clay (<2µm) (%)**	**Methylene Blue Index (meq/100g)**	**Specific Gravity**
Oil Sands Fluid Fine Tailings (FFT)	3.9	52	32	85	43	7.5	2.2
Edgar Plastic Kaolin (EPK) Clay*	-	52	31	98	61	-	2.65

*Data obtained from (Sorta et al. 2016)

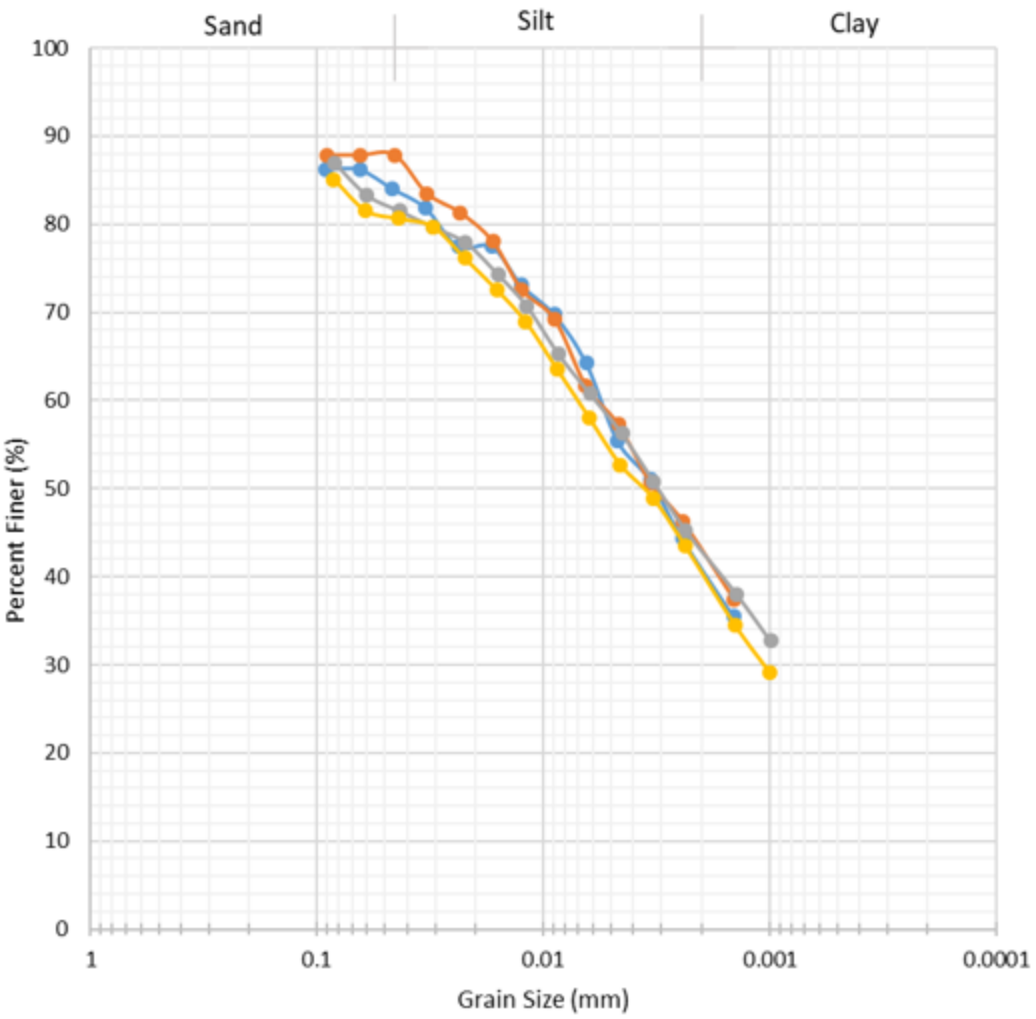

Figure 7 - Oil Sands Fluid Fine Tailings Hydrometer Results

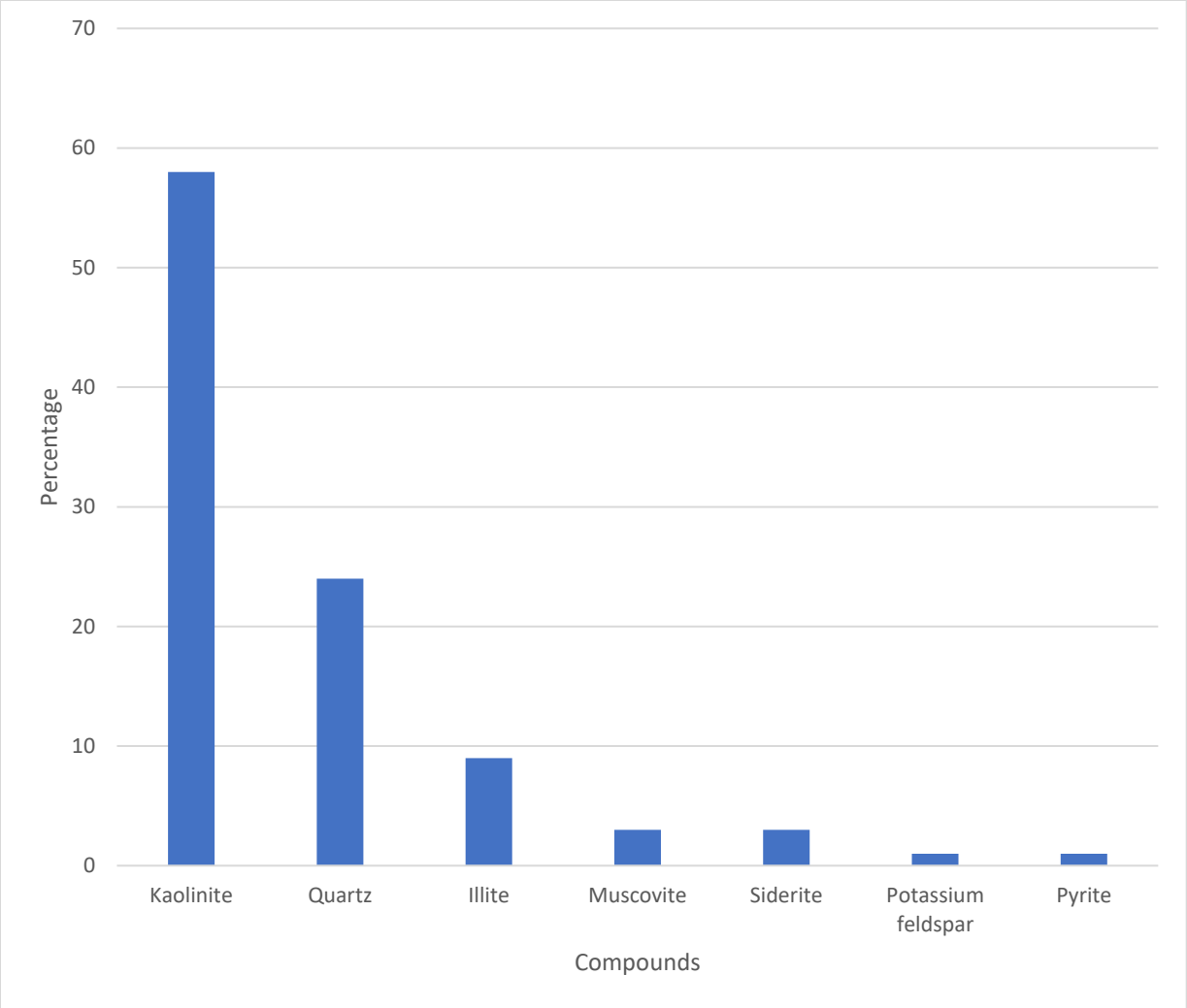

Figure 8 - X-Ray Diffraction Analysis of Oil Sands FFT

The FFT was flocculated using an A3338 flocculant at a dosage of 785g/T. The flocculant type and dosage were selected based on the work of other researchers (Fisseha et al. 2018). The purpose of this research was not to determine the optimum flocculant dosage for this material, though that process is outlined in (Mizani et al. 2013). The procedure for preparing the flocculated tailings is given below.

1. Prepare a 0.4% solution w/w of A3338 flocculant using recycled process water
2. Dilute FFT to approximately 35.5% solids using recycled process water
3. Measure desired quantity of FFT to be flocculated (batches were approximately 4kg for these tests)
4. Submerge impeller into FFT and set mixing speed (250 rpm)
5. Add required flocculant dosage based on calculations

6. Allow flocculant to mix for 10 seconds
7. Remove impeller and allow mixture to sit
8. Decant water using syringe

A photograph of a flocculated FFT mixture is shown below in Figure 9. The mixture begins releasing water immediately after flocculation. In these tests, the prepared material sat for less than 24 hours before loading into the centrifuge consolidation cells, to reduce the amount of water released. Solids content samples were taken immediately after material was loaded into the centrifuge consolidation cells.

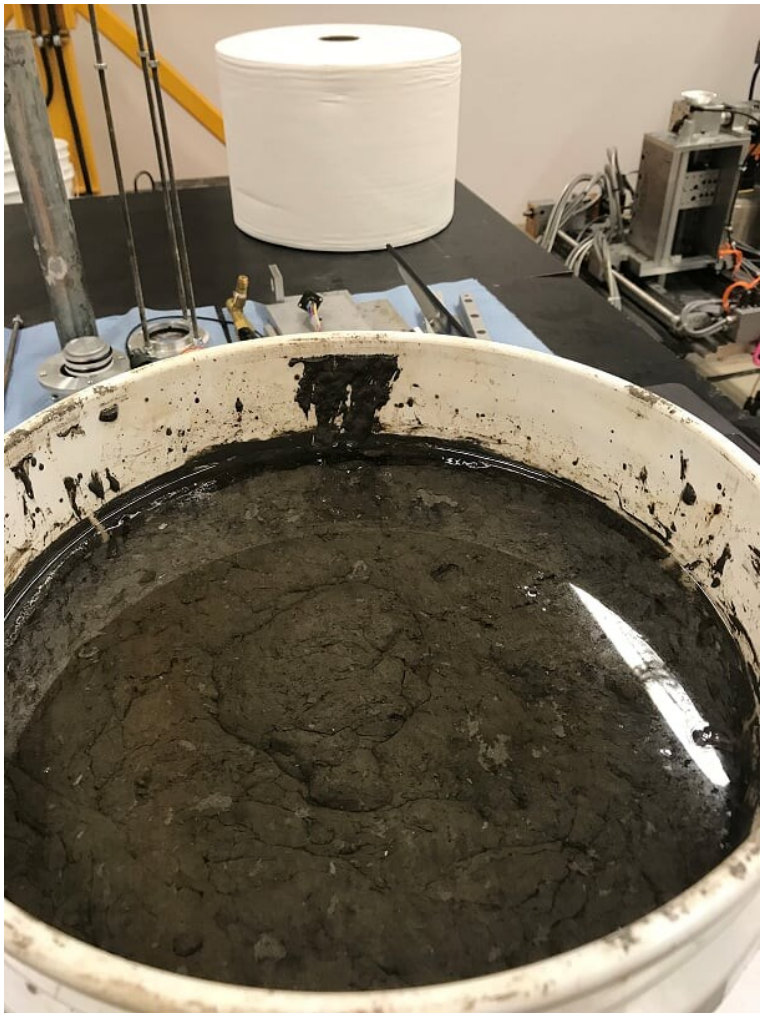

Figure 9 - FFT Mixture After Flocculation

3.2 Testing Equipment

3.2.1 Geotechnical Centrifuge

A 2.0m beam centrifuge located at the University of Alberta in Edmonton, Alberta, Canada, was utilized for these tests. The geotechnical centrifuge is part of the Geomechanical Experimental Research Facility (GeoREF) at the University of Alberta. The beam centrifuge is capable of accommodating payloads up to 500kg at 100-G and 330kg at 150-G, with maximum dimensions up to 0.6m wide x 0.8m length x 0.9m height. The payload is balanced by adjusting the position of the counterweights (before testing) and fine oil balancing (in-flight). An industrial programmable logic controller (PLC), located in the centrifuge control room controls the speed, automatic balancing, drive overload protection, access to interlocks, and start and stop sequences (Zambrano-Narveaz and Chalaturnyk 2014). The centrifuge room is monitored via two wall-mounted web cameras and the test package is monitored by an HD camera mounted to the centrifuge test platform. The centrifuge room is climate controlled by an air conditioning system. A schematic of the centrifuge is shown in Figure 10. Further details of the centrifuge and the centrifuge facility can be found in (Zambrano-Narveaz and Chalaturnyk 2014) and (TBS 2012).

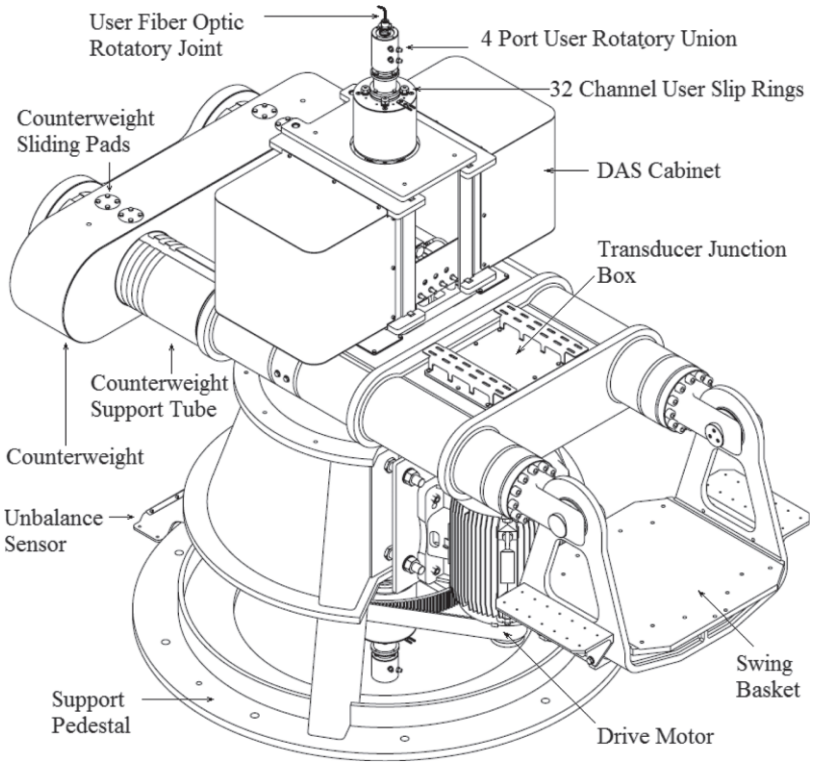

Figure 10 - Geotechnical Centrifuge Schematic (from (Zambrano-Narveaz and Chalaturnyk 2014)

3.2.2 Consolidation Cell and Instrumentation

The consolidation cell used in these tests consists of a plexiglass cylinder with a height of 297mm and an internal diameter of 177mm. The plexiglass cylinder is encased in an aluminum frame built to withstand the high G-level in the centrifuge. The consolidation cell is instrumented with six pore pressure ports; one port on the base of the cell and five attached to the cell wall. In these tests, the base pore pressure port and the top port on the cell wall were not used. Scales are attached to the inside wall of the consolidation cell and are used to monitor interface settlement in-flight via an externally mounted HD camera. The consolidation cell is shown in Figure 11. The steps for preparing the consolidation cells prior to loading the test materials is outlined below.

1. Cells are cleaned and dried
2. Filter paper is placed on the base of the cell and glued to the pore pressure ports along the wall of the cell
3. Cell is filled with de-aired water and allowed to sit for 24-hours
4. Water is forced through pore pressure port location to remove entrapped air*
5. Saturated pore pressure sensors are attached to the wall of the cell*
6. Water is vacuumed from the cell
7. Material is loaded into the cell
8. Loaded cells are secured to the centrifuge platform

   *In the layered fill tests, pore pressure ports were re-saturated as the material reached the port locations. Refer to Figure 12.

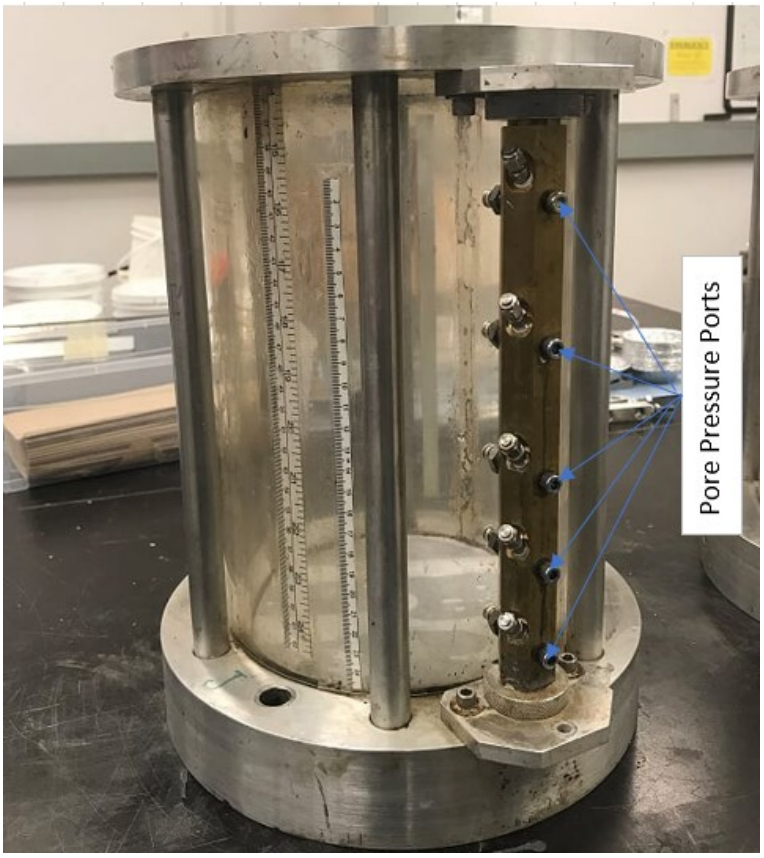

Figure 11 - Consolidation Cell Used in Centrifuge Tests

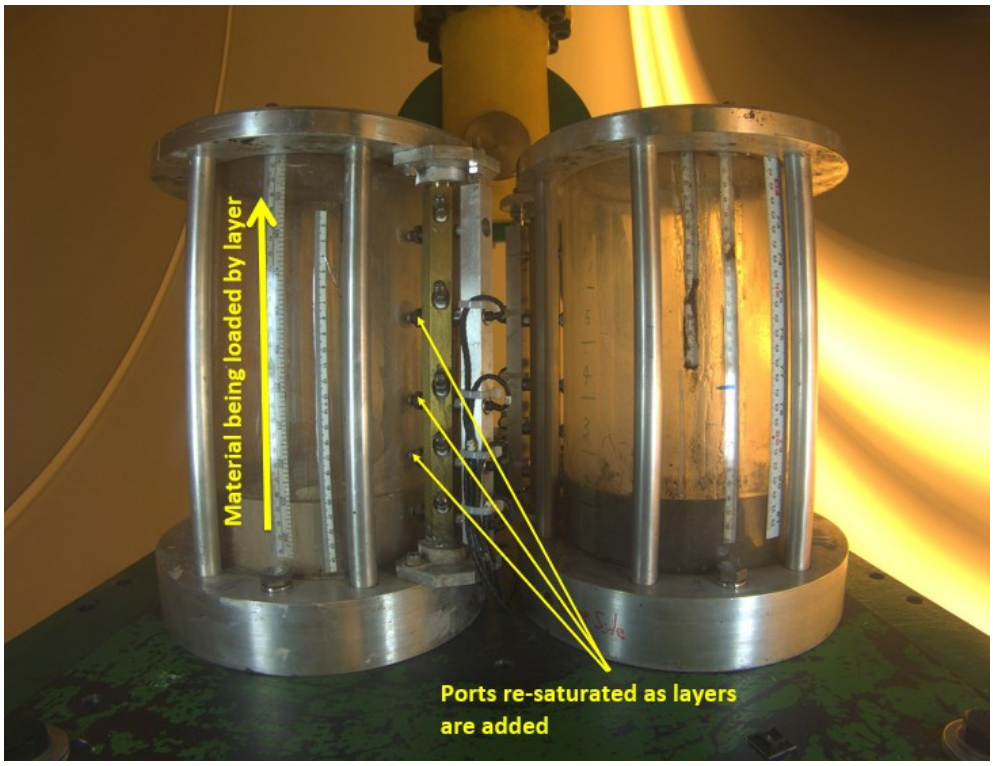

Figure 12 - Pore Pressure Port Saturation in Layered Fill Tests

3.2.3 Dispenser

A custom dispenser designed and built by the GeoREF team at the University of Alberta was used for adding layers of FFT in the layered fill tests. The dispenser was designed for more difficult materials that do not easily flow, such as treated oil sands tailings products. The dispenser offers some distinct advantages when used in the layered fill tests:

- Shearing of material is minimized (important when handling flocculated materials)
- Easier to measure desired quantity of material
- Minimal disturbance of underlying material (previous layers within the consolidation cell).

A schematic of the dispenser is shown in Figure 13.

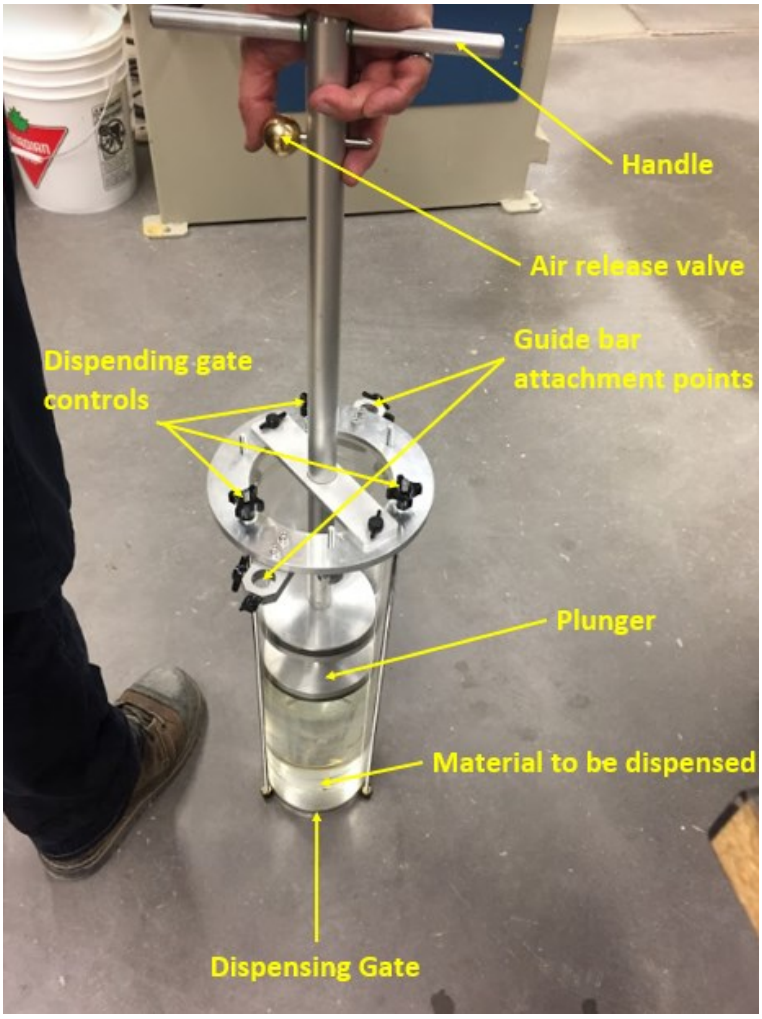

Figure 13 - Material Dispenser Schematic

3.3 Sampling Techniques

This section will cover the laboratory sampling techniques used in the experimental program. The procedures for settlement monitoring and void ratio/solids content profile generation are outlined.

3.3.1 Settlement Monitoring

Interface settlement of the centrifuge models is tracked in-flight with an HD camera that is attached to the centrifuge swing platform. The camera takes photos at desired intervals and saved to an external computer for viewing. Scales attached to the inside wall of the centrifuge test cells allow interface settlement to be monitored. The scales are discernable up to 0.5mm from the photos. Scale readings are taken at set intervals and matched to the elapsed time (photos are time stamped) to generate the settlement curves. The camera setup and example photos obtained during flight are shown in Figure 14 and Figure 15.

In the single fill tests, photos were taken every ten seconds for the first hour of flight time, and every five minutes for the rest of the flight time. In the layered fill tests, photos were taken every thirty seconds for the first hour of flight time, and every five minutes for the rest of the flight time. The photo capture interval was increased in the layered fill tests as the shorter interval in the single fill tests did not provide additional data required to generate the settlement curves.

Figure 14 - HD Camera Setup for Interface Settlement Monitoring

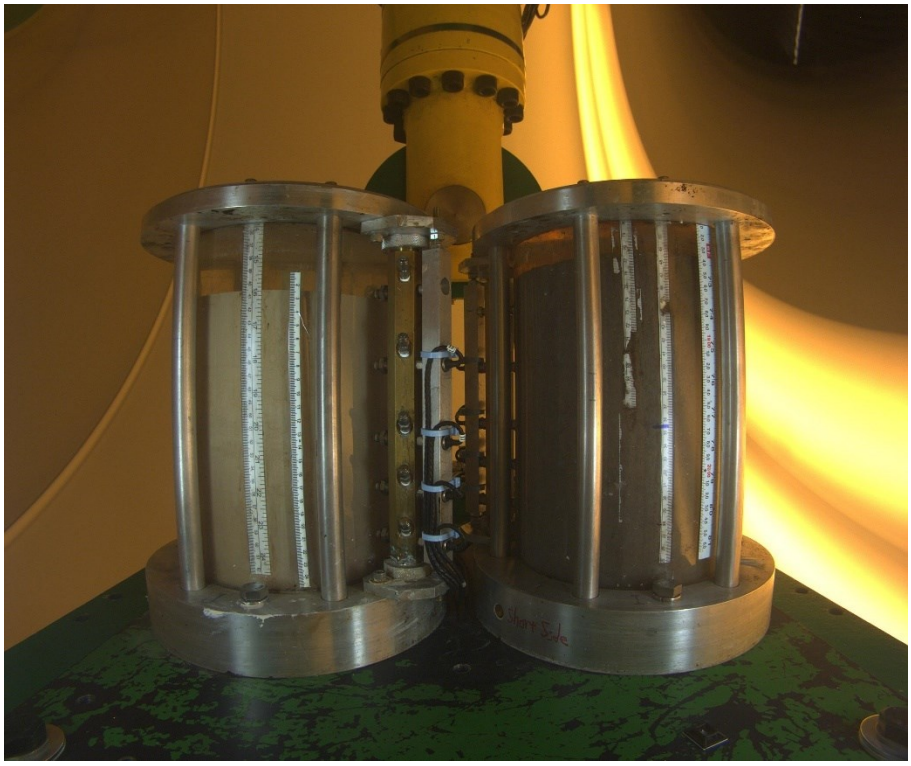

Figure 15 - Sample Photo Obtained In-flight from HD Camera (Single Fill Tests)

3.3.2 Void Ratio and Solids Content

Void ratio and solids content profiles are not monitored in-flight but are instead obtained from sampling the model after centrifuge flight. The procedure for obtaining the void ratio/solids content profiles from the centrifuge model is outlined below. The sampling technique is shown in Figure 16.

1. Consolidation cell is removed from centrifuge platform and carefully transported to work bench
2. Top cap of consolidation cell is removed, and release water is decanted using a syringe
3. Push tubes are inserted into sample
4. Surrounding material is excavated
5. Push tubes are removed from consolidation cell
6. Material is extruded from the push tubes in six equal layers
7. Individual samples are placed in tins, weighed, and oven dried at 105°C for 24 hours
8. Dried samples are weighed again to determine solids content

Figure 16 - Push Tube Sampling Technique

a) Push tubes are inserted into sample, b) Push tubes are removed from sample, c) Samples are extruded from push tube in six equal layers, d) Samples are dried in oven to obtain solids content

The push-tube sampling technique is a potential source of error in these tests. When inserting the push tubes into the sample, the sample compresses or expands depending on its final density after consolidation. More dense samples, such as the kaolinite, expand from push tube insertion; less dense samples, such as FFT, compress from insertion. This phenomenon is demonstrated in Figure 17. As shown, the final height of the sample obtained from the push tube is not the same as the final height of the consolidated material within the cell. Therefore, the location of each sample node from the push tube samples may not match its location before sampling within the consolidation cell. To minimize this error, the height of the push tube samples is adjusted to match the undisturbed height within the consolidation cell before sampling. Error still exists from this technique because this compression/expansion of material from push tube insertion is likely non-uniform throughout the entire depth of the sample.

Figure 17 - Push Tube Sampling Technique in Consolidated FFT (Left) and Kaolinite Slurry (Right)

3.4 Centrifuge Test Procedures

3.4.1 Selection of Centrifuge Test Conditions

The geotechnical centrifuge allows researchers to investigate numerous geotechnical problems with physical modelling. Selection of the G-level and centrifuge flight time can be scaled to field-scale prototypes to achieve the desired conditions. In this experimental program, the centrifuge test conditions (G-level and flight time) were chosen to replicate the filling of an oil sands tailings pond. An example filling schedule of an oil sands tailings pond is shown below in Figure 18. In this example tailings pond, material is deposited annually until the targeted final elevation is reached. Layered fill tests completed in this thesis attempt to model this continuous addition of material, and the subsequent settlement that occurs once the final elevation is reached. Field data for this example tailings pond is not available, and no attempt is made to compare field settlement with settlement values obtained from centrifuge consolidation tests. The example tailings pond fill schedule simply provides a reasonable framework with which to base the centrifuge consolidation tests on.

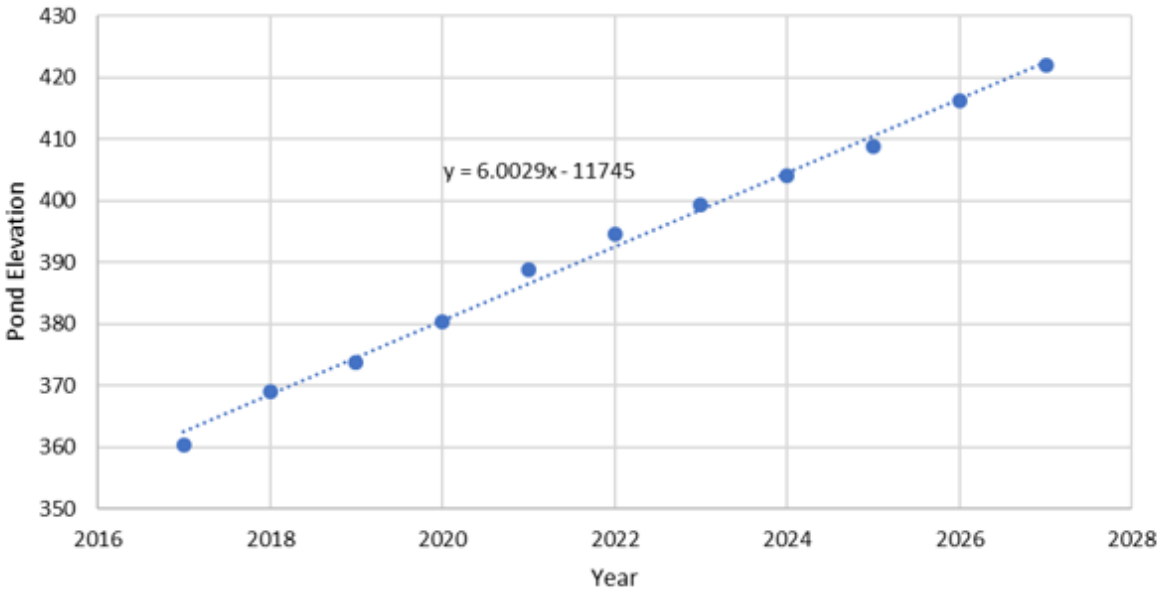

Figure 18 - Example Tailings Pond Fill Schedule

3.4.2 Single Fill Test Procedure

In the single fill tests, the consolidation cells were filled with material prior to being loaded on the centrifuge platform. Once loaded on the centrifuge platform, the centrifuge was started and run for the targeted amount of time. The test conditions for the single fill tests are summarized below in Table 3.

Table 3 - Single Fill Test Conditions

Material	**Initial Solids Content (%)**	**Model Height (cm)**	**Model Time (hrs)**	**Prototype Height (m)**	**Prototype Time (years)**
Kaolinite	39.0	28.4	24.1	28.4	27.6
Tailings	42.6	27.3	24.1	27.3	27.6

The single fill tests were completed in a single flight of the centrifuge without stopping. The centrifuge required approximately 15 minutes of ramp-up time when starting to complete self-balancing

procedures. This ramp-up time was accounted for when converting between total model time and total prototype time. The recorded G-level with time is shown below in Figure 19.

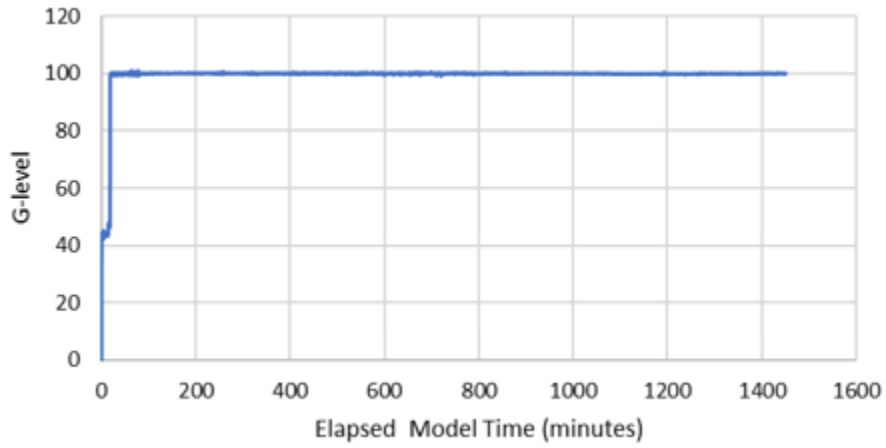

Figure 19 - G-level in Single Fill Tests

3.4.3 Layered Fill Test Procedure

In the layered tests, consolidation cells were filled layer-by-layer until the targeted amount of material had been added (six layers total). The centrifuge was run for approximately one hour between layers, to allow individual layers to consolidate. The procedure for adding each layer is outlined below.

1. Allow centrifuge to come to a complete stop
2. Take readings of material and water interface heights
3. Remove top cap from centrifuge consolidation cells
4. Decant water using syringe
5. Add new layer of material
6. Reinstall top cap of consolidation cells
7. Restart centrifuge

The kaolinite slurry was added by funneling in the targeted quantity of material (measured by volume). This process is shown in Figure 20. The tailings material was added to the consolidation cells by using the dispensing device previously described. The procedure for using the tailings dispenser is outlined in Figure 21.

Figure 20 - Funneling Kaolinite Slurry into Consolidation Cell

Figure 21 - Dispensing Tailings Material to the Consolidation Cell

a) Material is added to the dispenser, b) Dispenser is secured to the consolidation cell, c) Dispenser shown inside consolidation cell, d) Dispensed material in the consolidation cell

The addition of a new layer took approximately fifteen minutes to complete with two workers (grad student and lab technician). No appreciable rebound of either material was observed due to stopping the centrifuge between layer additions. The test conditions for the layered fill tests are summarized below in Table 4. The FFT model was spun for an additional 24-hours in the layered tests to allow more settlement to occur. The loading schedule for kaolinite and tailings are shown in Table 5 and Table 6, respectively.

Table 4 - Layered Fill Test Conditions

Material	**Initial Solids Content (%)**	**Model Height (cm)**	**Model Time (hrs)**	**Prototype Height (m)**	**Prototype Time (years)**
Kaolinite	38.4	29.1	23.9	29.1	24.2
Tailings	42.3	28.8	48.4	28.8	51.4

Table 5 - Kaolinite Loading Schedule for Layered Test

Kaolinite Loading Schedule	**Model Height Added (cm)**	**Model Time (hours)**	**Prototype Height Added (m)**	**Prototype Time (years)**
Layer 1	5.2	1.0	5.2	1.1
Layer 2	4.8	1.0	4.8	1.1
Layer 3	4.9	1.0	4.9	1.1
Layer 4	4.8	1.0	4.8	1.1
Layer 5	4.8	1.0	4.8	1.1
Layer 6	4.6	(Spun to target time of 24 hrs)	4.6	24.2 (total)

Table 6 - Tailings Loading Schedule for Layered Test

Tailings Loading Schedule	Model Height Added (cm)	Model Time (hours)	Prototype Height Added (m)	Prototype Time (years)
Layer 1	4.9	1.0	4.9	1.1
Layer 2	4.7	1.0	4.7	1.1
Layer 3	4.5	1.0	4.5	1.1
Layer 4	5.5	1.0	5.5	1.1
Layer 5	4.9	1.0	4.9	1.1
Layer 6	4.3	(Spun to target time of 48 hrs)	4.3	51.4 (total)

Because the centrifuge had to be stopped and started to add each new material layer, G-level fluctuated during testing. Although changes in G-level meant the material experienced changes to its self-weight, no appreciable rebound of the material was observed when the centrifuge was stopped. The G-level was monitored continuously throughout the layered tests, as shown in Figure 22. A drop in the recorded G-level is shown during addition of layers in the early stages of testing, and again at the 24-hour mark, where the kaolinite model was removed from the centrifuge platform. The recorded G-level does not drop to 1-G, as data collection stops when the centrifuge is stopped.

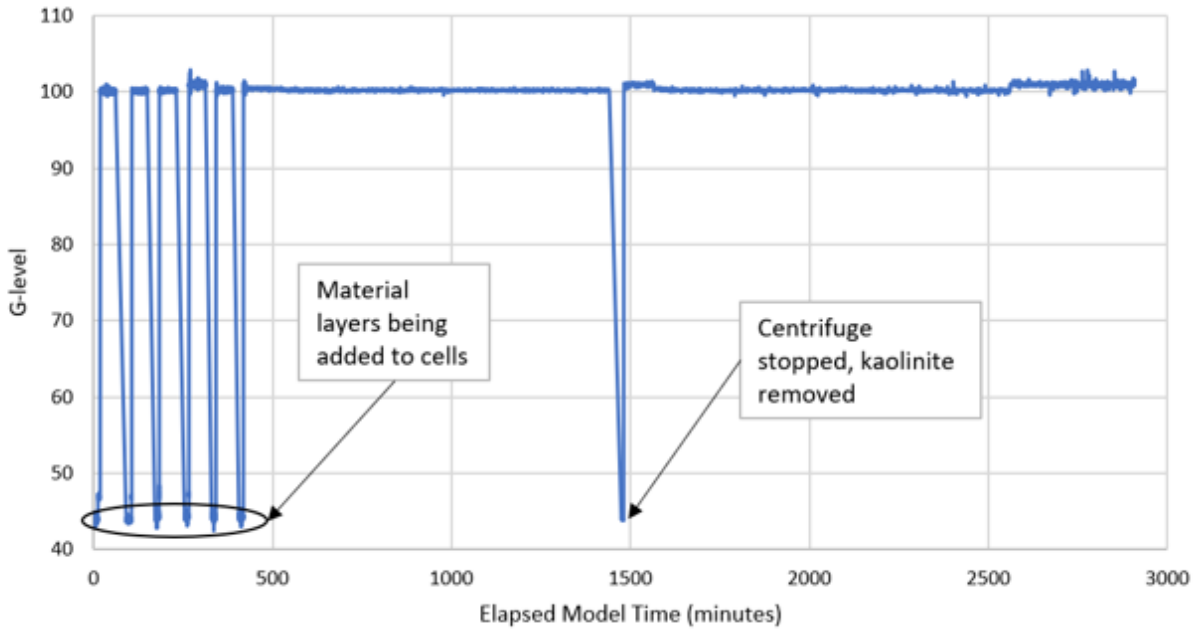

Figure 22 - G-level in Layered Fill Tests

3.5 Numerical Modelling Technique

Large strain numerical modelling software (FSCA, https://www.fscasoftware.com/) was used to generate settlement curves for both the kaolinite and FFT samples. To run this software, void ratio-effective stress curves and permeability-void ratio curves must be obtained. The void ratio-effective stress relationship is an exponential relationship given by the following equation:

$$e = A\sigma'^{B} \quad [3]$$

Where e is the void ratio, σ' is the effective stress, and A and B are curve fitting parameters. The permeability-void ratio relationship is an exponential relationship given by the following equation:

$$k = Ce^{D} \quad [4]$$

Where k is the permeability, e is the void ratio, and C and D are curve fitting parameters. The curve fitting parameters (A, B, C, D) can be obtained from large strain consolidation tests, directly from the centrifuge, or a combination of the two (Sorta et al. 2016).

3.5.1 Selection of Model Input Parameters

The numerical model input parameters for kaolinite were derived using a combination of centrifuge results and LSCT results. The void ratio-effective stress curves were generated using the centrifuge tests conducted as part of this thesis, and the permeability-void ratio curves were obtained from LSCT results

from other researchers. The void ratio-effective stress curve for kaolinite is shown in Figure 23 and the permeability-void ratio curve is shown in Figure 24 (Sorta et al. 2016).

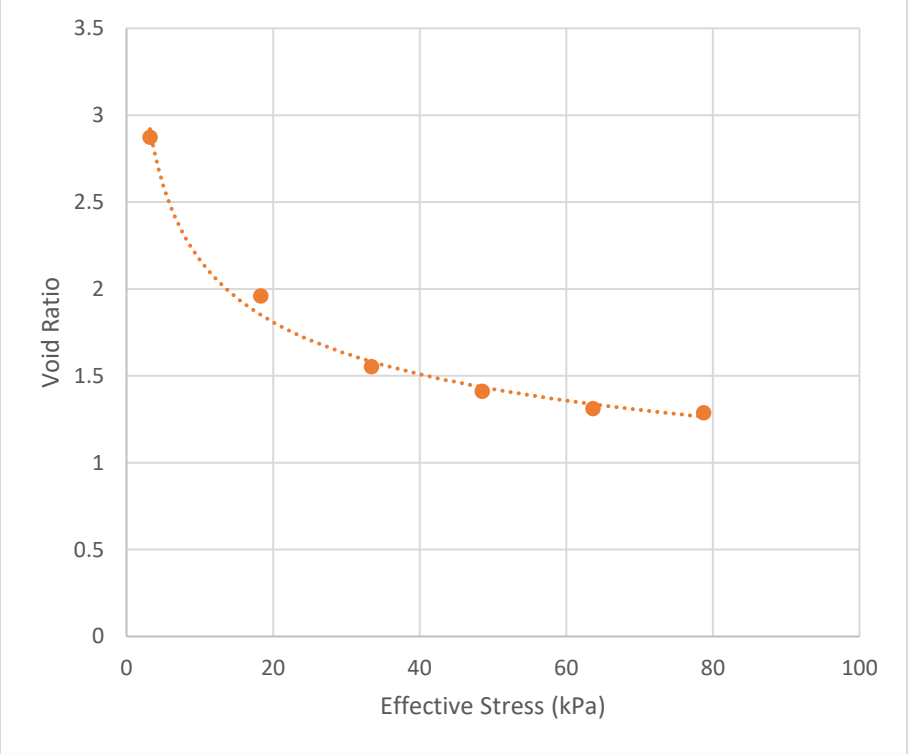

Figure 23 - Kaolinite Void Ratio-Effective Stress Curve

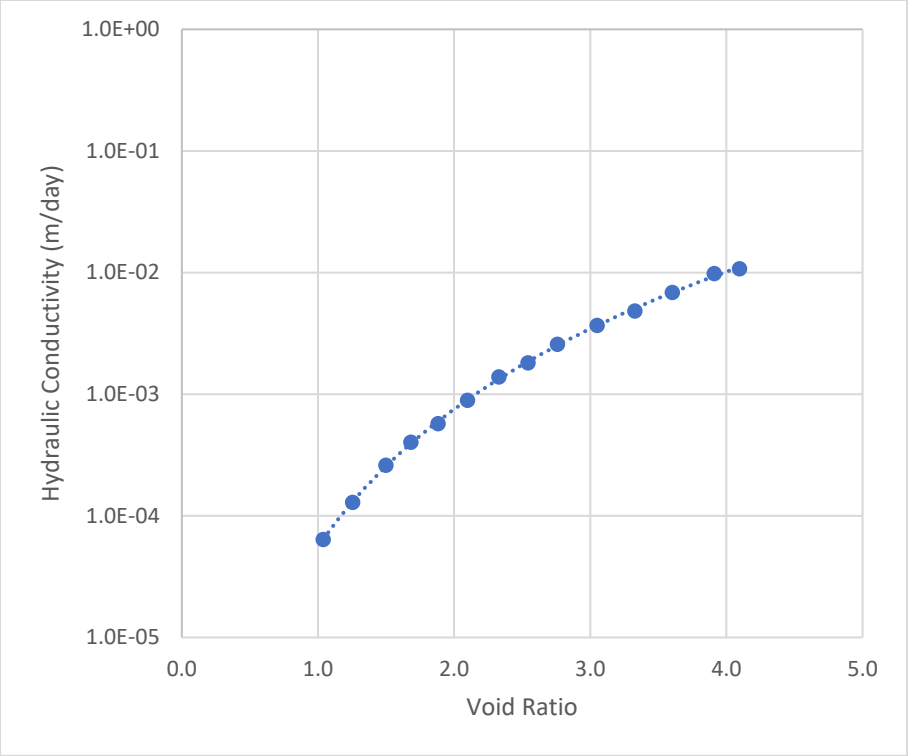

Figure 24 - Kaolinite Permeability-Void Ratio Curve (Sorta, 2016)

The void ratio-effective stress curve and permeability-void ratio curve for the FFT used in this thesis were obtained from (Fisseha et al. 2018). (Fisseha et al. 2018) conducted several LSCT tests on the same material used in this thesis at different flocculant dosages. Those results are shown in Figure 25 and Figure 26.

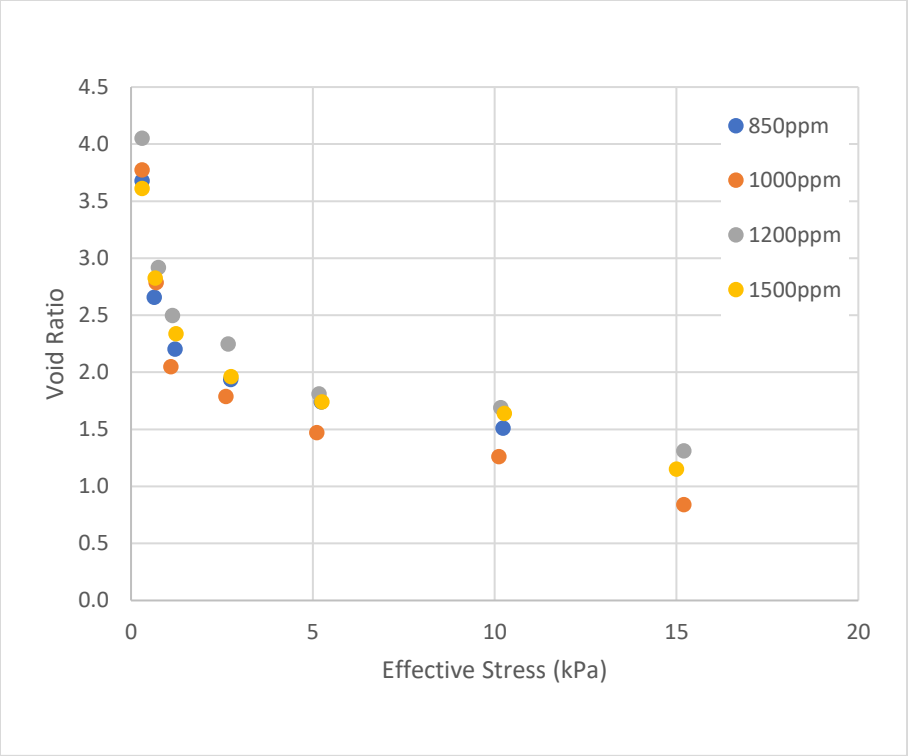

Figure 25 - FFT Void Ratio-Effective Stress Curves (Fisseha et al. 2018)

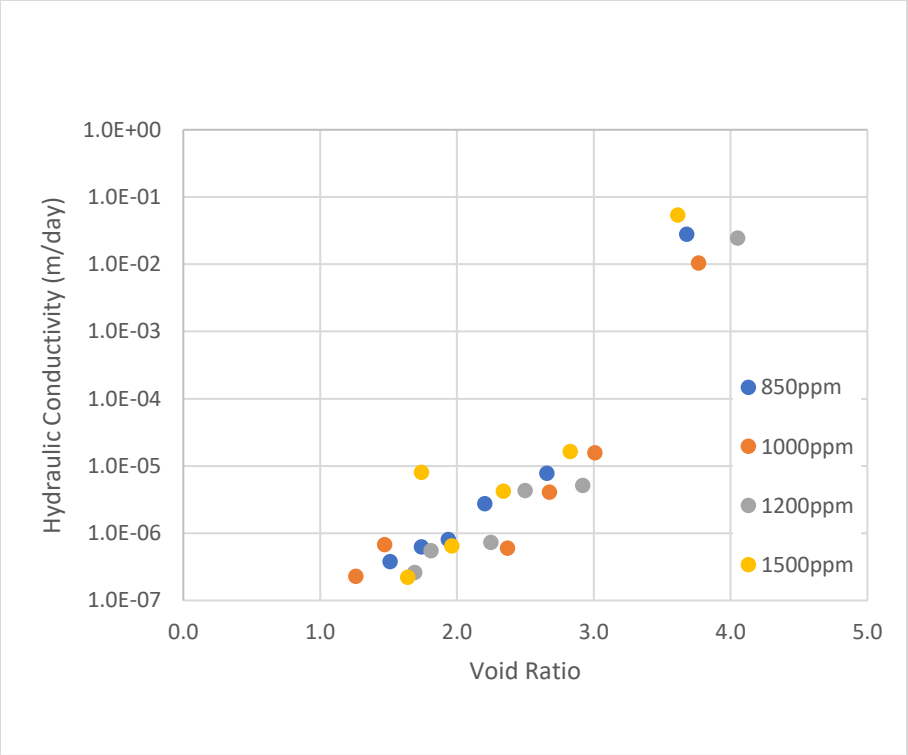

Figure 26 - FFT Permeability-Void Ratio Curve (Fisseha et al. 2018)

A summary of the chosen model input parameters is given in Table 7.

Table 7 - FSCA Large Strain Numerical Model Input Parameters

Material	A (kPa)	B (no units)	C (m/day)	D (no units)
Kaolinite	3.956	-0.261	6.000×10^{-5}	3.756
FFT	2.514	-0.237	5.000×10^{-10}	12.131

4 Test Results

This chapter will present all results from the experiments.

4.1 Settlement Curves

In-flight photos of the consolidation cells are shown in Figure 27. The settlement progression is visible in these photos. The settlement curves for the kaolinite slurry tests and FFT tests are shown in Figure 28 and Figure 29, respectively. Results are presented at the prototype scale (time in years, height in meters). A summary of the total settlement for the kaolinite and FFT is given in Table 8 and Table 9, respectively. The percent settlement is calculated as the change in height (settlement) divided by the original height.

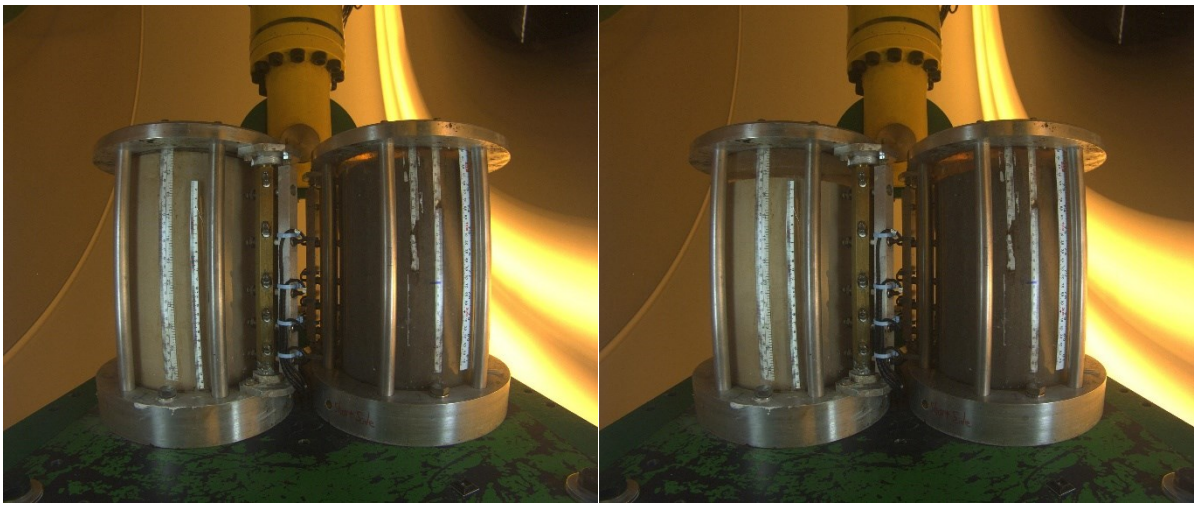

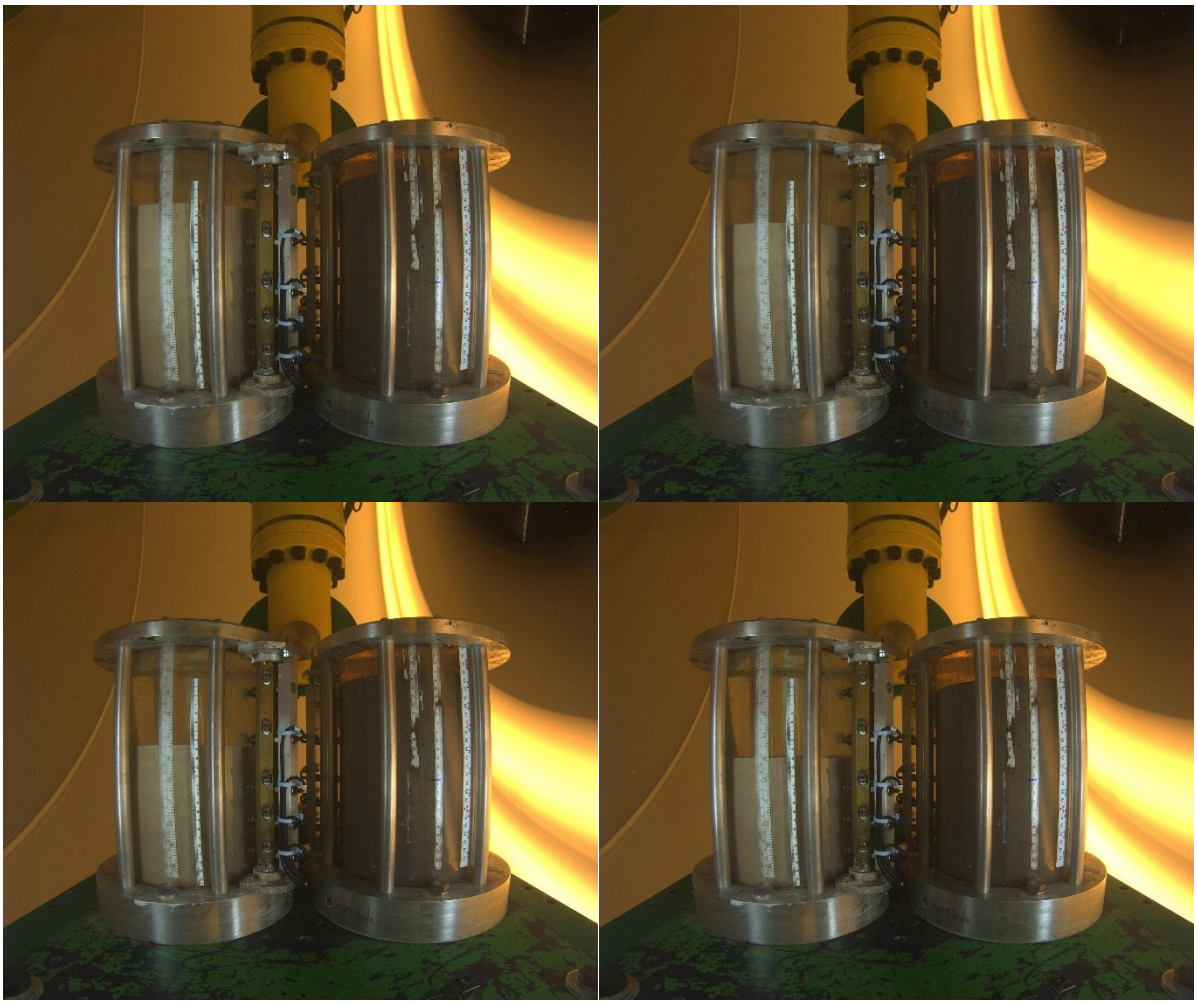

Figure 27 - In-flight Photos of Consolidation Cells Showing Progression of Settlement with Time (kaolinite shown on the left, tailings on the right)

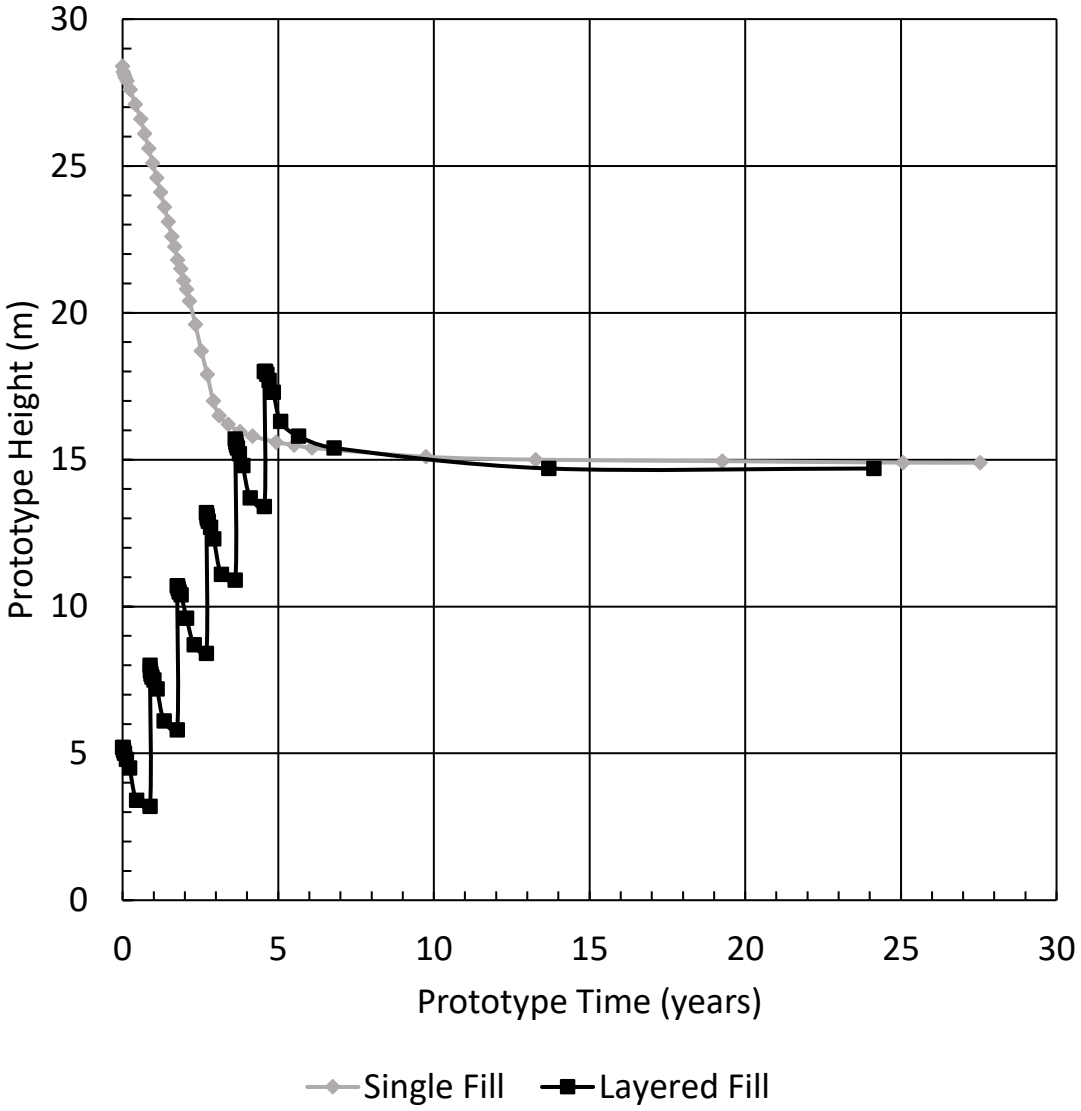

Figure 28 - Kaolinite Interface Settlement

Table 8 - Kaolinite Total Settlement

Test	Starting Height (m)	Final Height (m)	Total Settlement (m)	Total Settlement (%)
Kaolinite Single	28.4	14.9	13.5	47.5
Kaolinite Layered	29.1	14.5	14.6	50.2

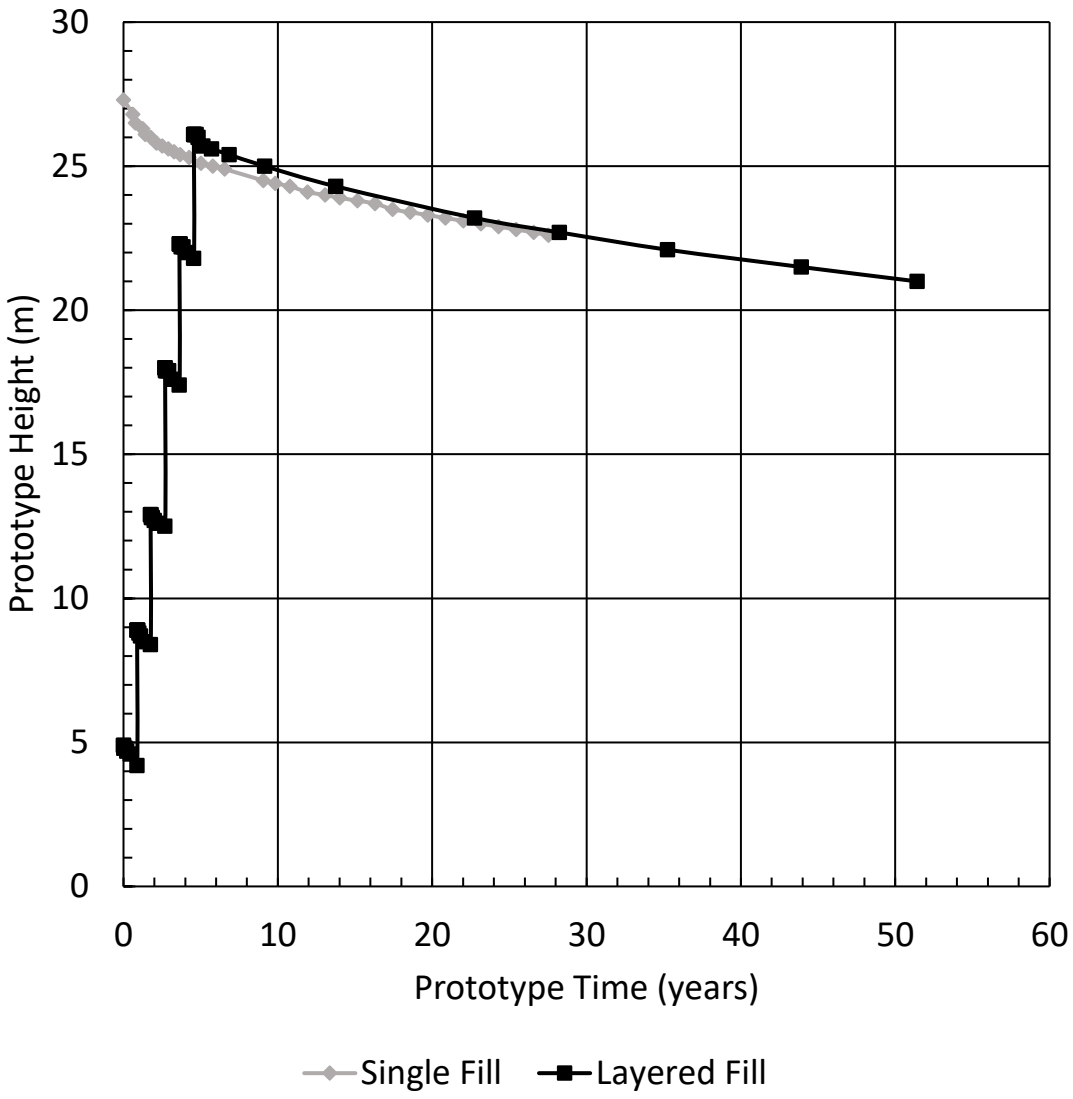

Figure 29 - FFT Interface Settlement

Table 9 - FFT Total Settlement

Test	Starting Height (m)	Final Height (m)	Total Settlement (m)	Total Settlement (%)
FFT Single (24hrs)	27.3	22.6	4.7	17.2
FFT Layered (24hrs)	28.8	23.0	5.8	20.1
FFT Layered (48hrs)	28.8	20.9	7.9	27.4

4.2 Void Ratio Profiles

The void ratio profiles at the end of testing are presented in Figure 30 and Figure 31 for the kaolinite and FFT samples, respectively. These profiles were generated using the sampling technique outlined in Chapter 3.

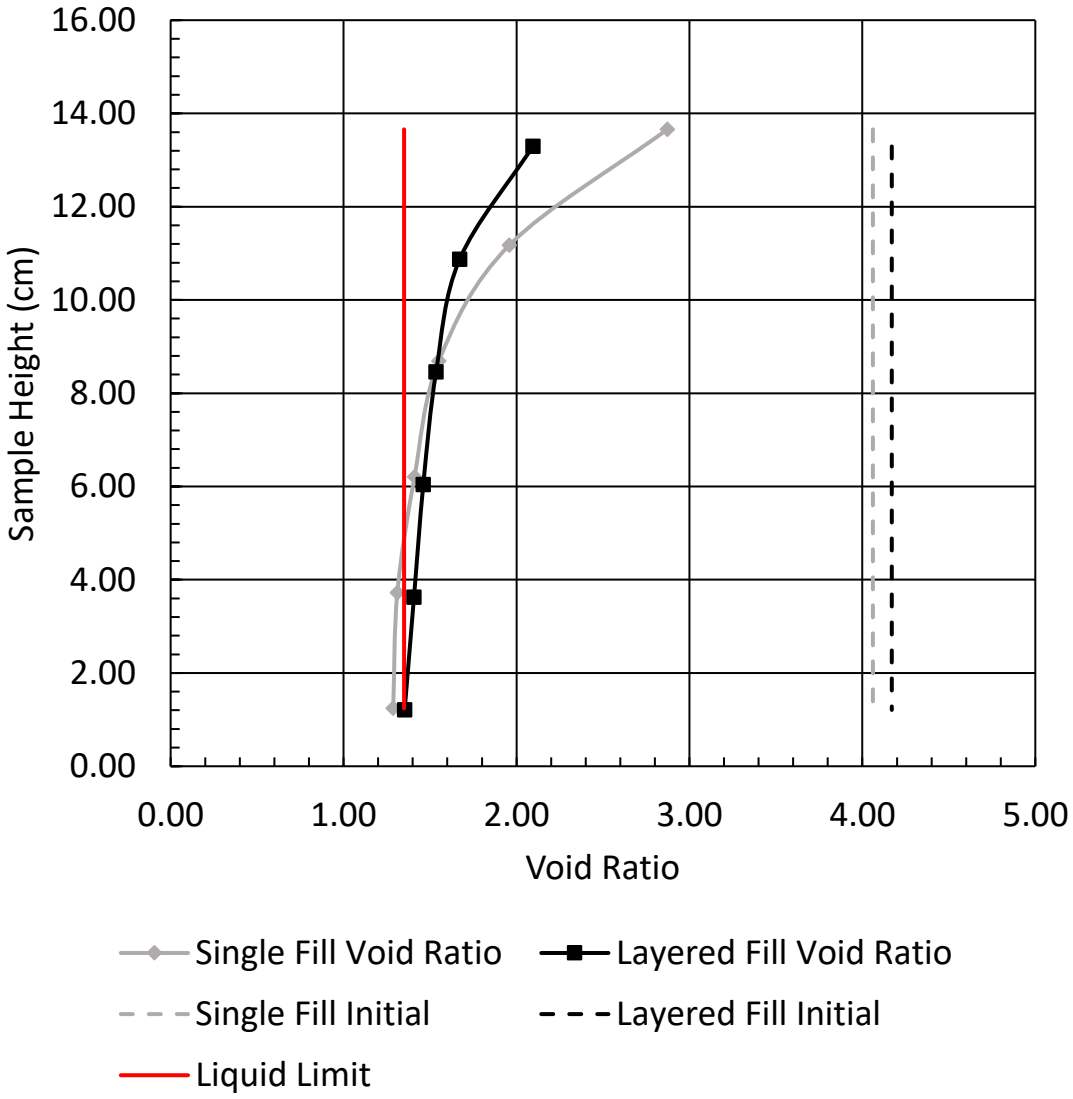

Figure 30 - Kaolinite Final Void Ratio Profiles

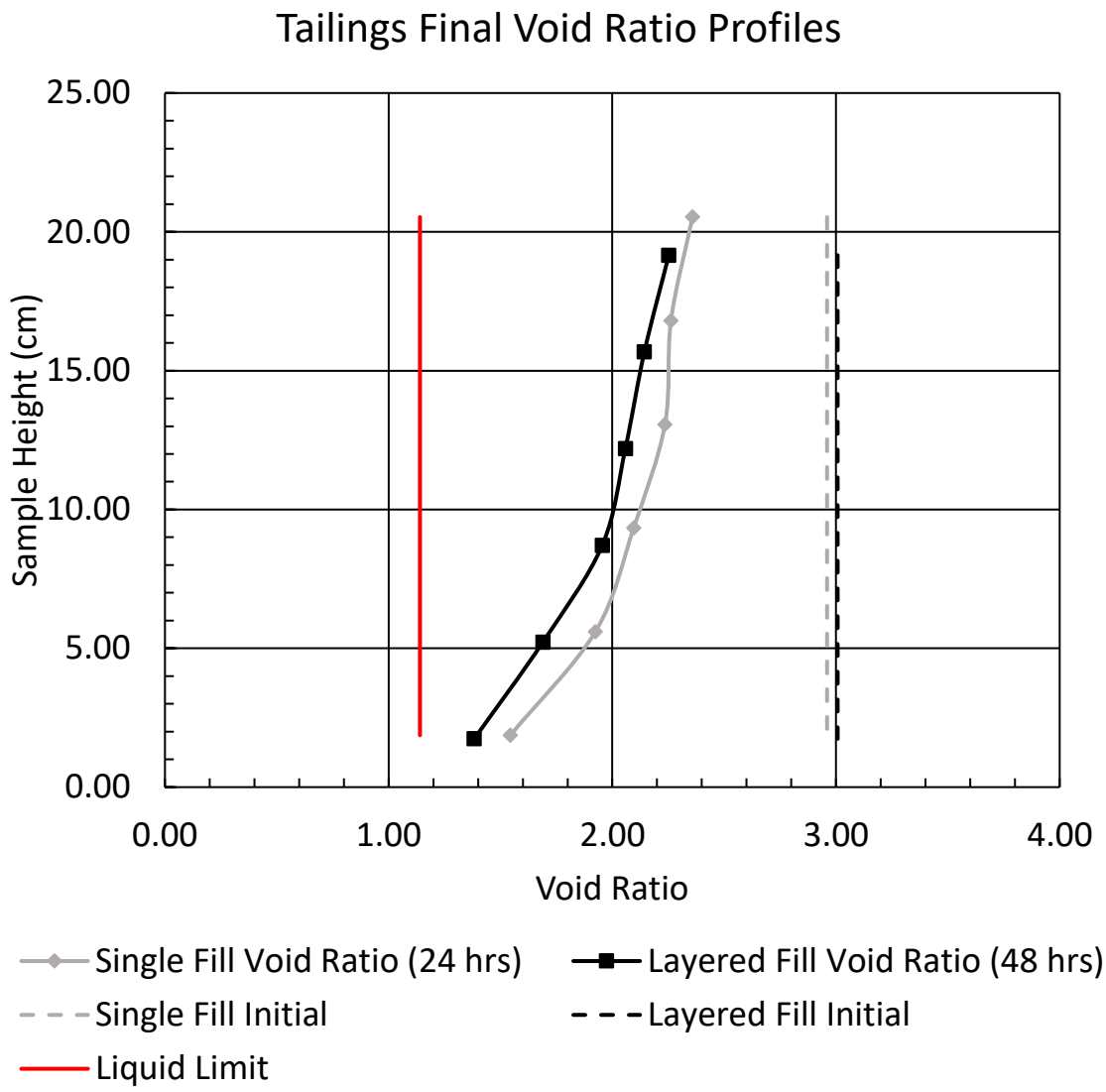

Figure 31 - FFT Final Void Ratio Profiles

4.3 Pore Pressure Profiles

The pore pressure profiles from the centrifuge tests are presented below in Figure 32 to Figure 39. Kaolinite are Figures 31 to 34 and FFT are Figures 35 to 38. Measured pore pressures were plotted with time from each pore pressure port, along with the hydrostatic values. In the figures, Port 1 refers to the bottom pore pressure port and Port 4 is the top port. Pore pressure dissipation with time graphs are also shown for each test (Figure 33, Figure 35, Figure 37, Figure 39). In the dissipation graphs, values are presented at interval times according to the elapsed prototype time, in years. In the pore pressure versus time plots, the hydrostatic value at each port is represented by a dashed line.

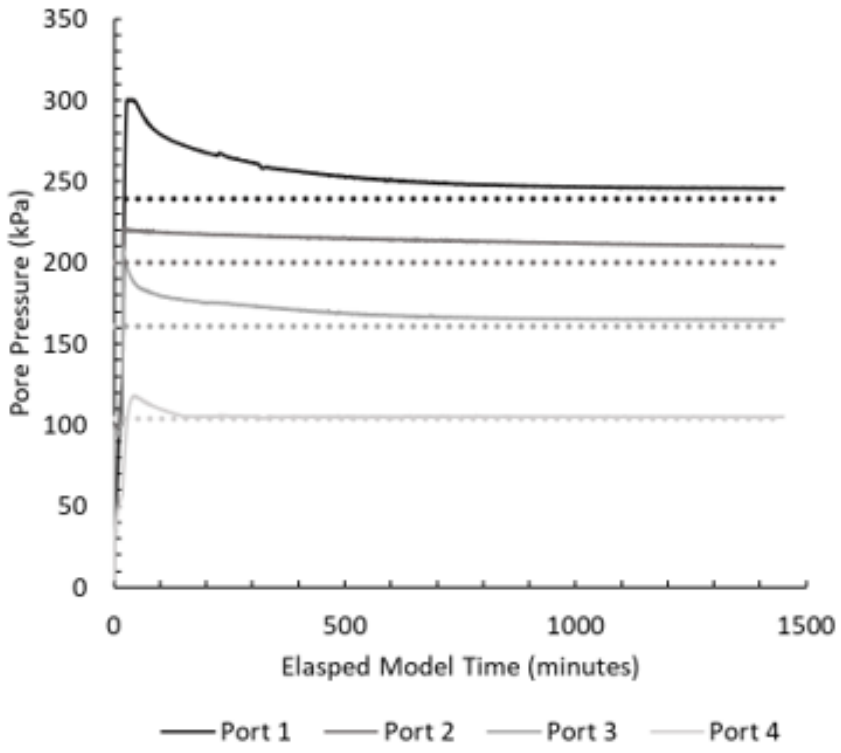

Figure 32 - Kaolinite Single Fill Pore Pressures

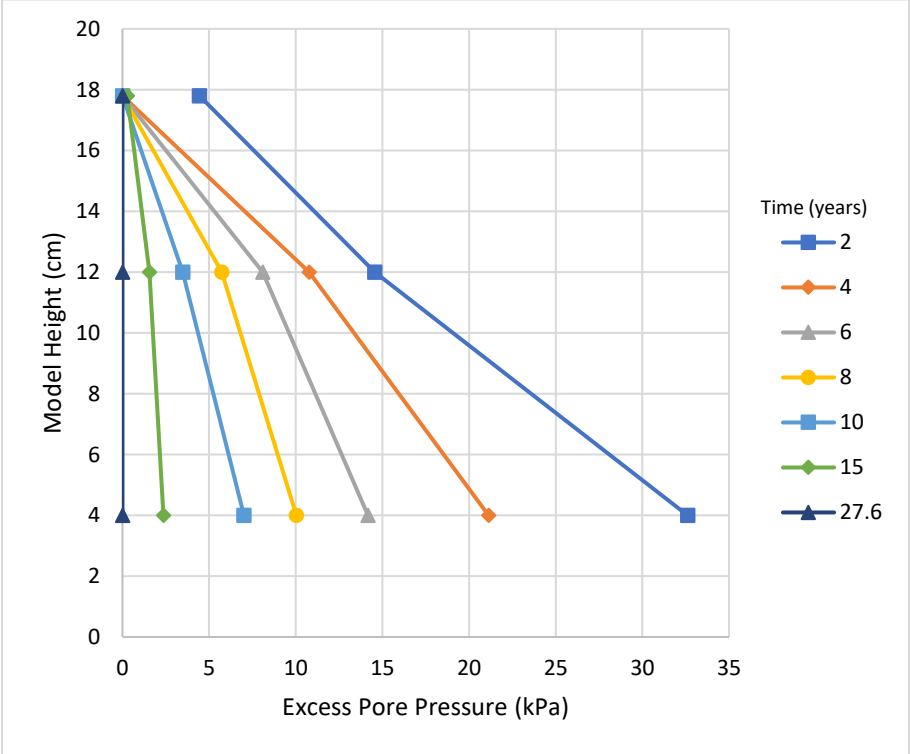

Figure 33 - Kaolinite Single Fill Pore Pressure Dissipation

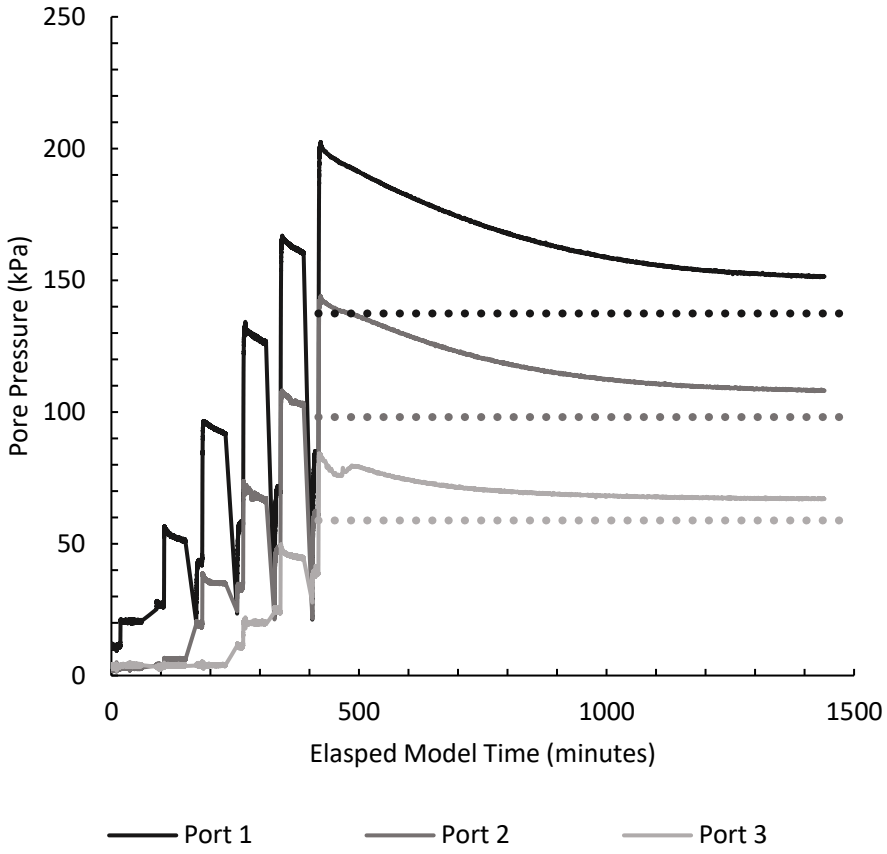

Figure 34 - Kaolinite Layered Fill Pore Pressures

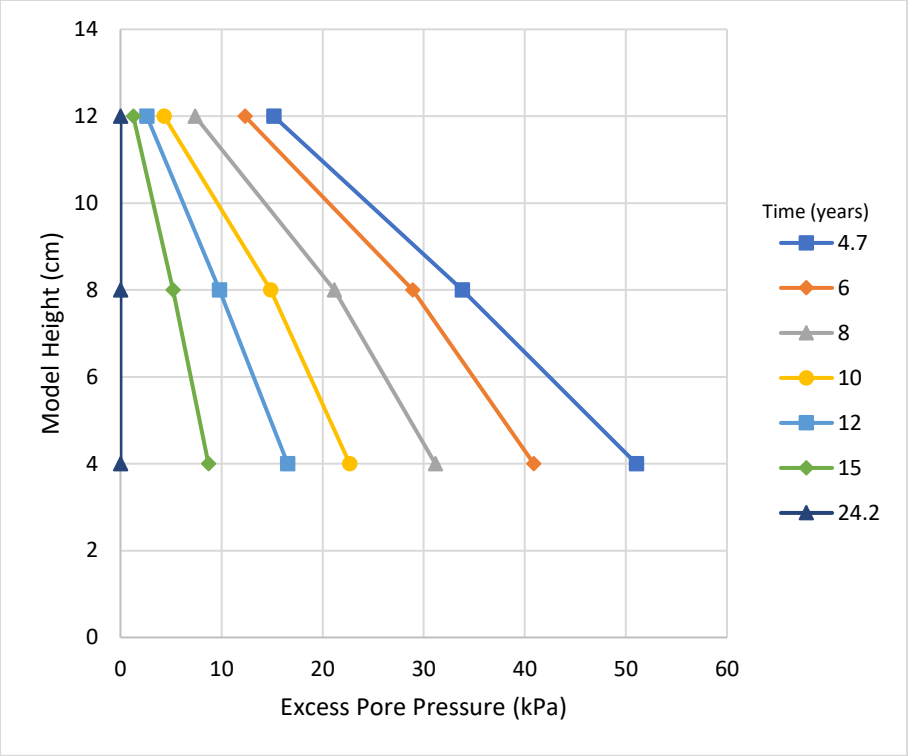

Figure 35 - Kaolinite Layered Fill Pore Pressure Dissipation

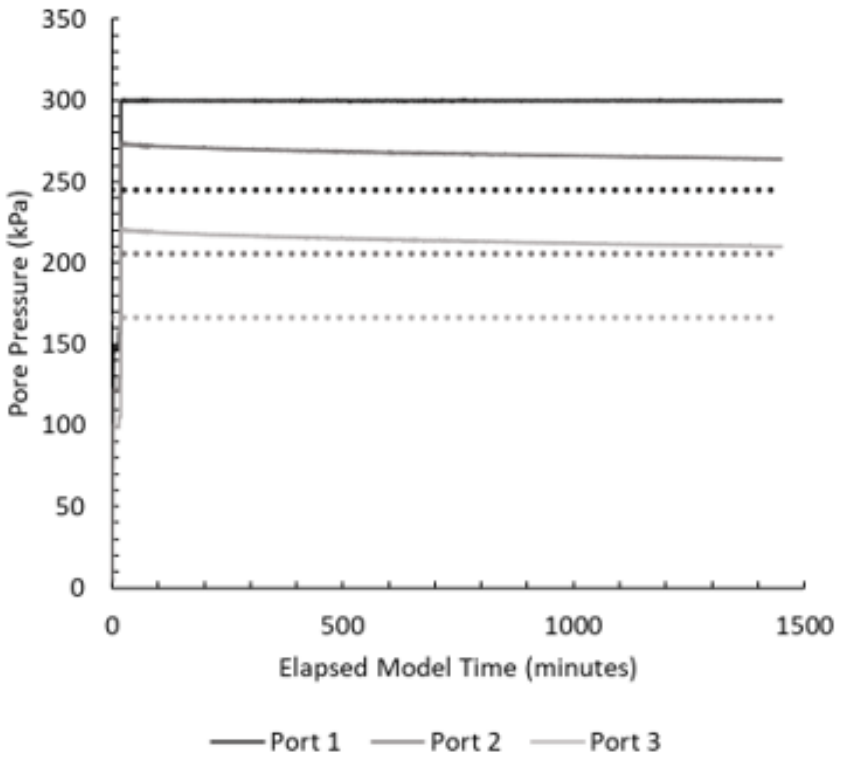

Figure 36 - FFT Single Fill Pore Pressures

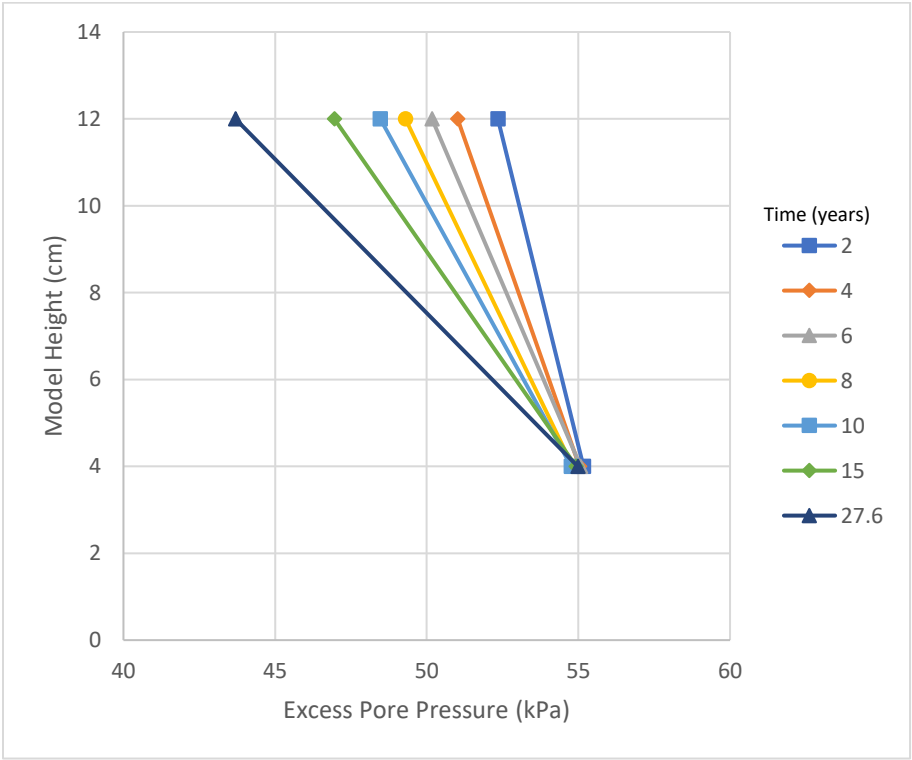

Figure 37 - FFT Single Fill Pore Pressure Dissipation

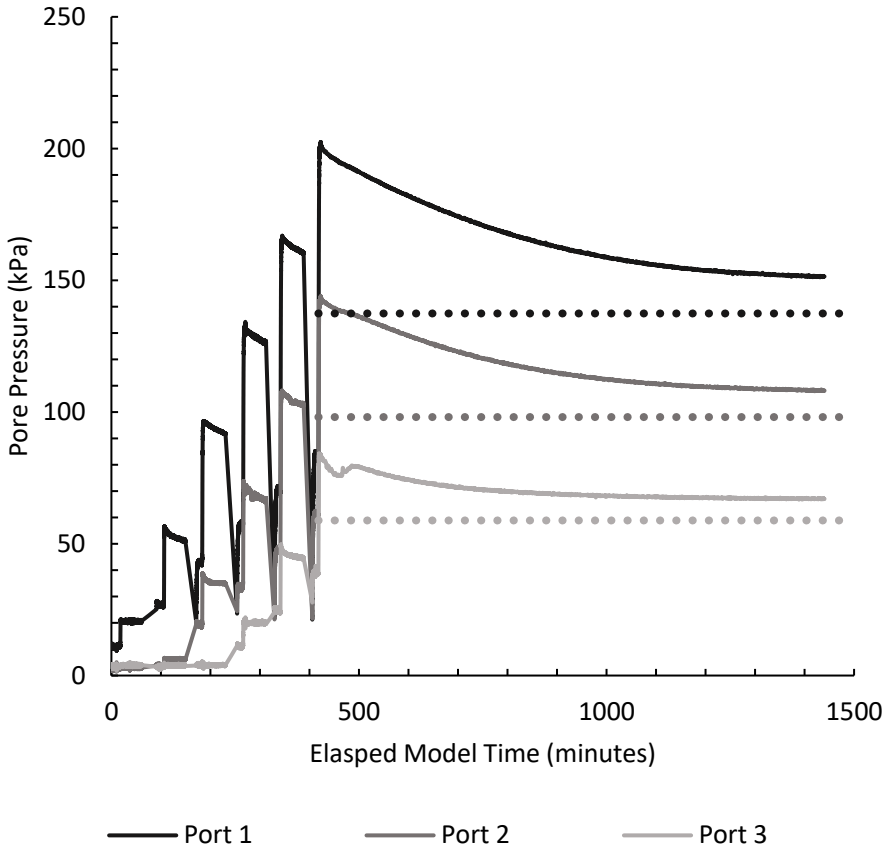

Figure 38 - FFT Layered Fill Pore Pressures

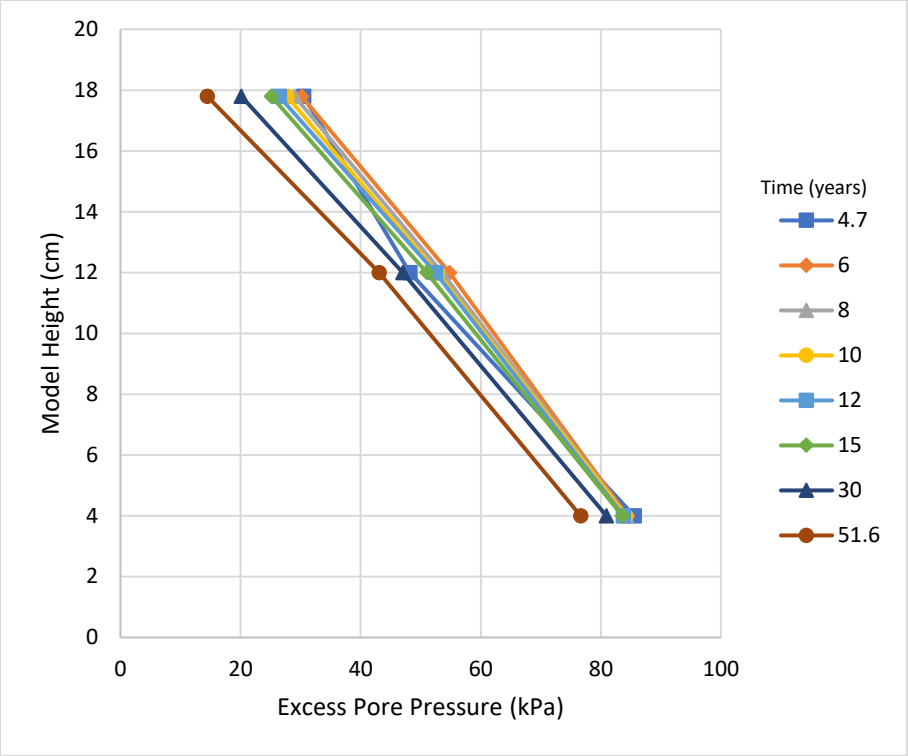

Figure 39 - FFT Layered Fill Pore Pressure Dissipation

4.4 Stress Profiles

Stress profiles were calculated for the kaolinite and FFT models from the collected lab data. The stress profiles for the kaolinite models includes total stress, pore pressure and effective stress curves. For the FFT tests, the total stress curves are plotted alongside a calculated hydrostatic pore pressure curve. However, because pore pressures did not adequately dissipate, measured pore pressures in the FFT models did not match the theoretical hydrostatic curve, and effective stress profiles were not able to be developed. Stress profiles for the kaolinite and FFT models are shown below.

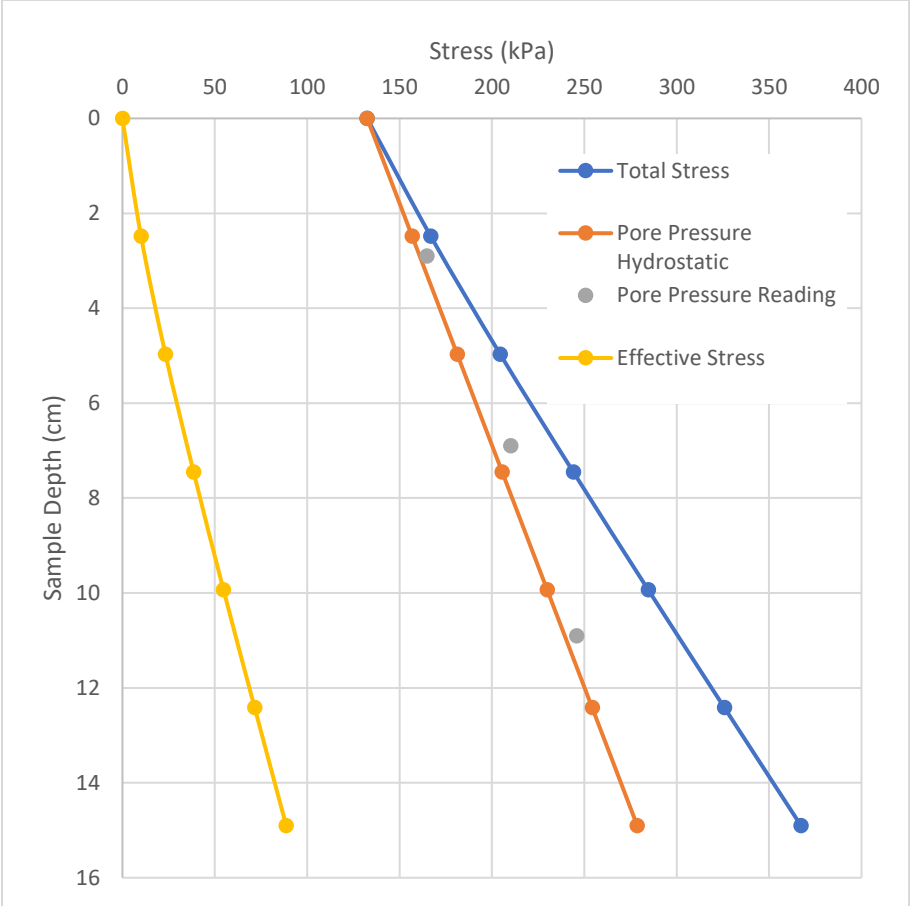

Figure 40 - Kaolinite Single Fill Stress Profile

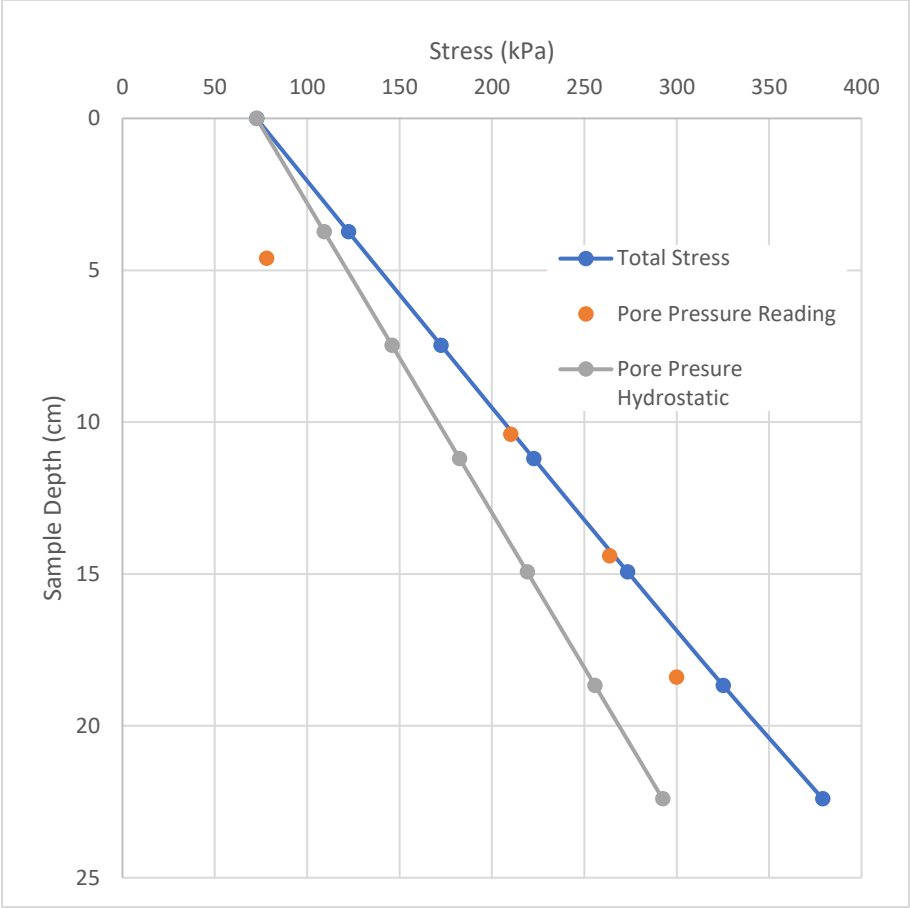

Figure 41 - FFT Single Fill Stress Profile

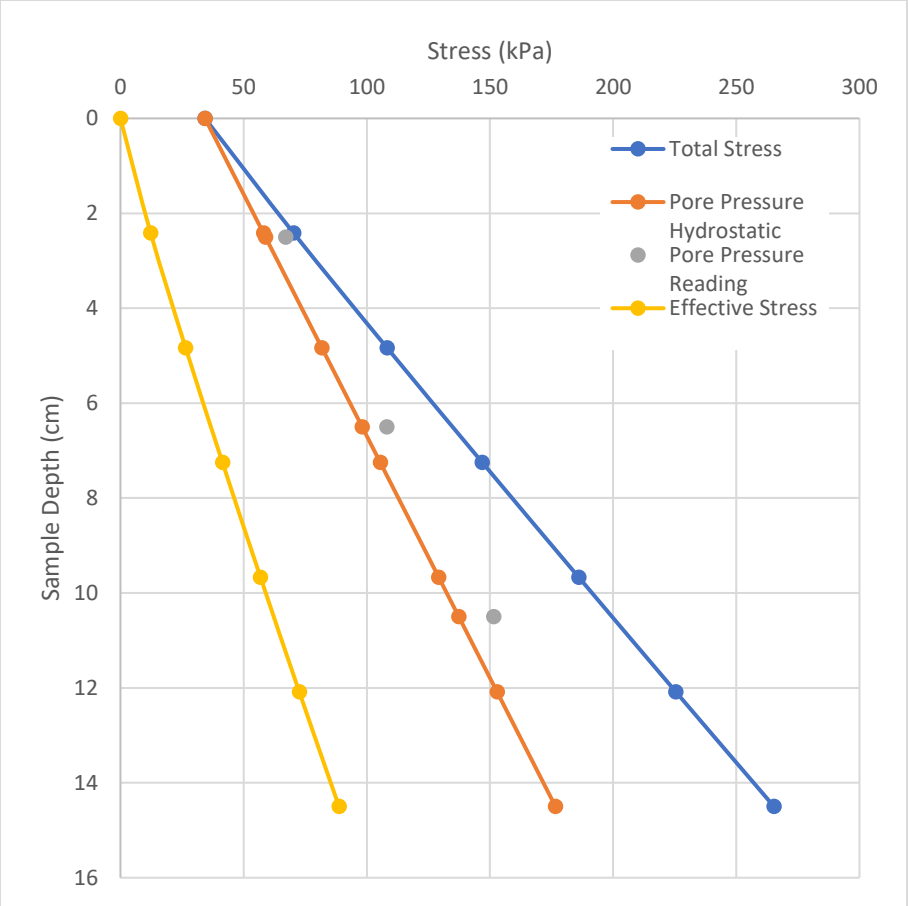

Figure 42 - Kaolinite Layered Fill Stress Profile

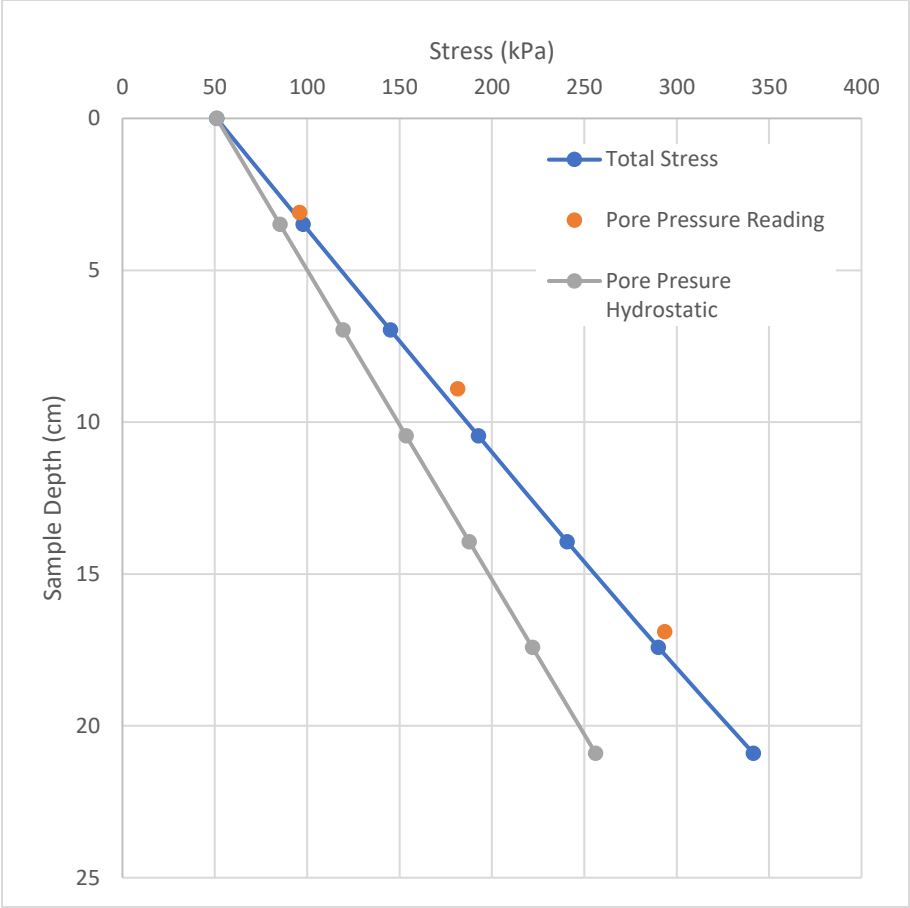

Figure 43 - FFT Layered Fill Stress Profile

4.5 Comparison with Numerical Models

The large strain numerical model was used to simulate the centrifuge tests and to compare results. The model input parameters used in the large strain numerical model (FSCA) are given in Chapter 3. The model input parameters were derived using a combination of centrifuge and LSCT results. Settlement curves were obtained from the numerical model, as well as final void ratio profiles. Those results are shown below in Figure 44 to Figure 49. Numerical model results are shown alongside centrifuge test results for comparison.

When running the numerical model, it was found that the settlement rate of both kaolinite and FFT was slower as compared to the centrifuge. To match the centrifuge results, the numerical model was re-run using an adjusted permeability function for each material. Adjusting the permeability led to better agreement between the numerical model and centrifuge test results. Further discussion on this can be found in Chapter 5.

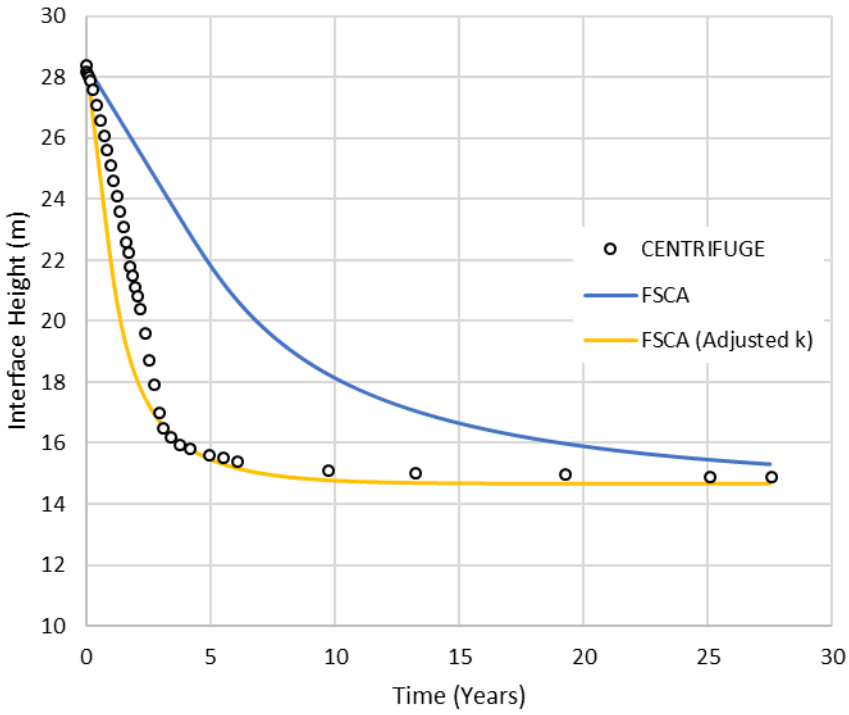

Figure 44 - Kaolinite Numerical Model Settlement Predictions (Single Fill)

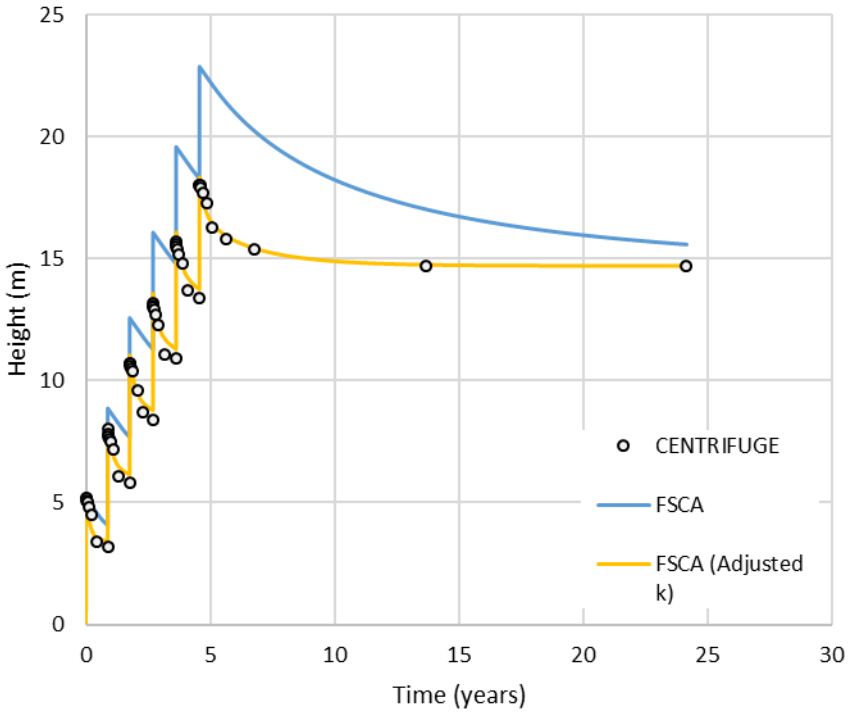

Figure 45 - Kaolinite Numerical Model Settlement Predictions (Layer Fill)

The final void ratio profiles for kaolinite is shown below. The centrifuge results were those obtained from the single fill kaolinite centrifuge test.

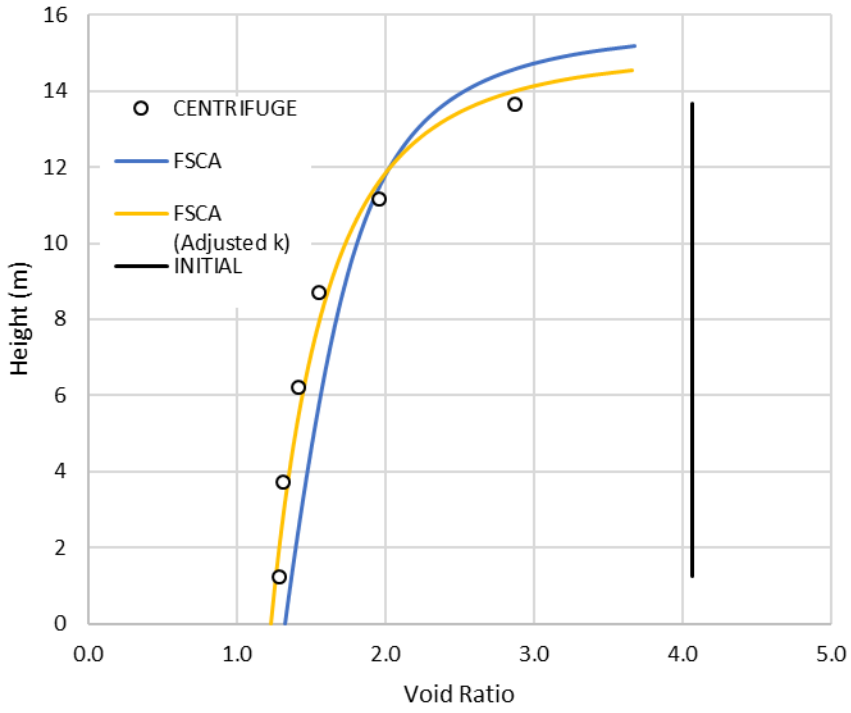

Figure 46 - Kaolinite Final Void Ratio Profile Prediction

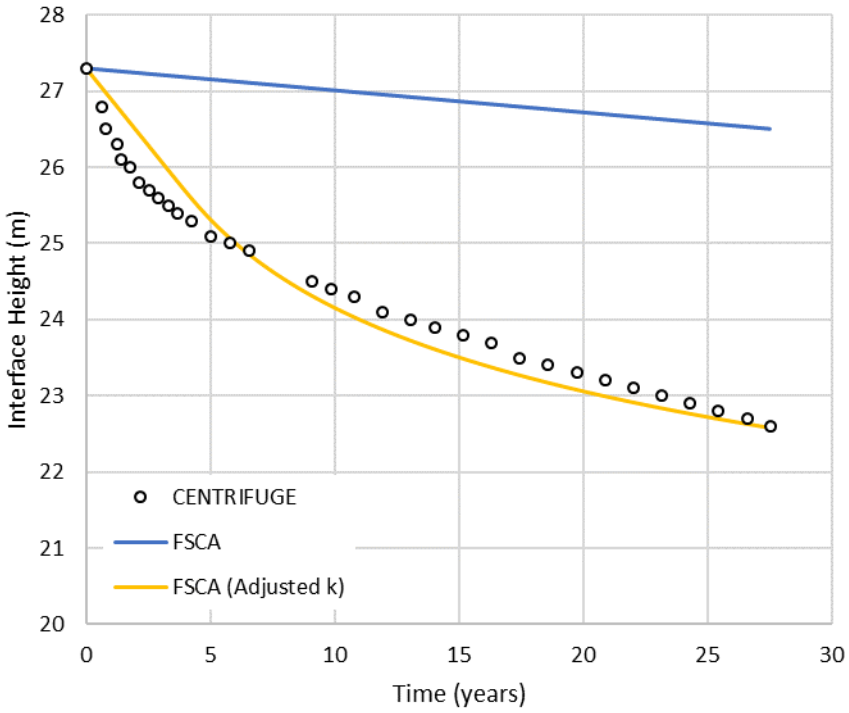

Figure 47 - FFT Numerical Model Settlement Predictions (Single Fill)

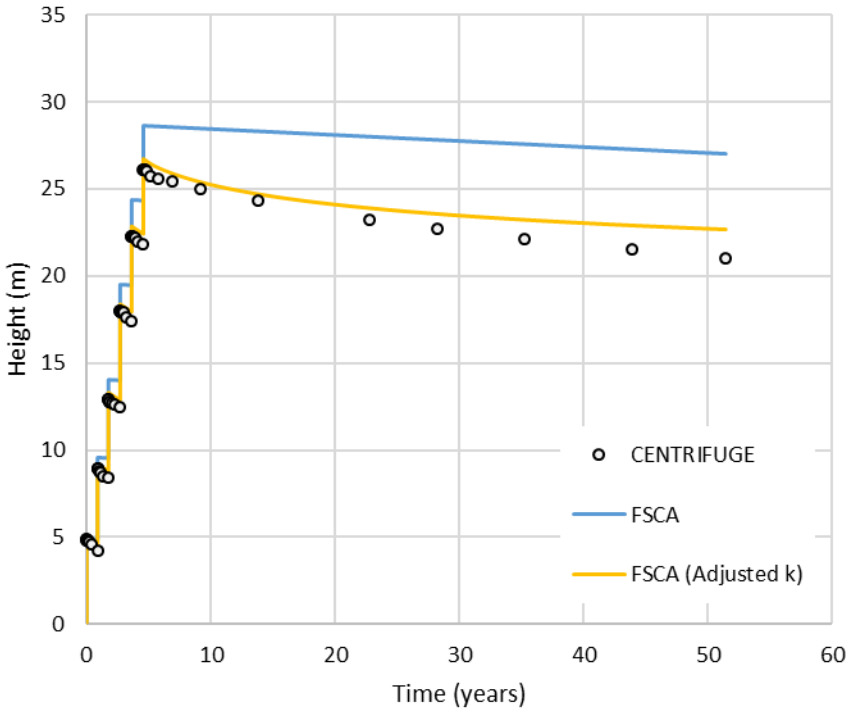

Figure 48 - FFT Numerical Model Settlement Predictions (Layer Fill)

The final void ratio profiles for FFT is shown below. The centrifuge results were those obtained from the single fill FFT centrifuge test.

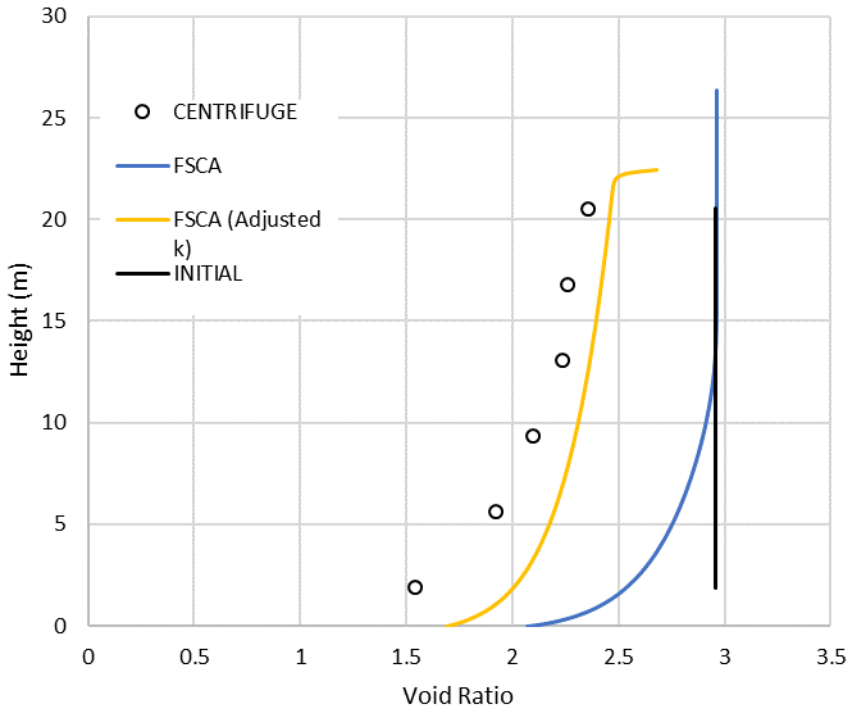

Figure 49 - FFT Final Void Ratio Profile Prediction

Excess pore pressure (PP) dissipation profiles were generated using the numerical model and compared to the results obtained from the centrifuge. The model results are those obtained using the adjusted permeability curve to more closely match the centrifuge results. Results are shown below in Figure 50 to Figure 53. The individual data points plotted on the graphs indicate centrifuge data, whereas the profiles generated using the numerical model are shown as lines. The number corresponds to the elapsed time the reading was taken (point C2 for example shows the pore pressures in the centrifuge model after two years of prototype elapsed time).

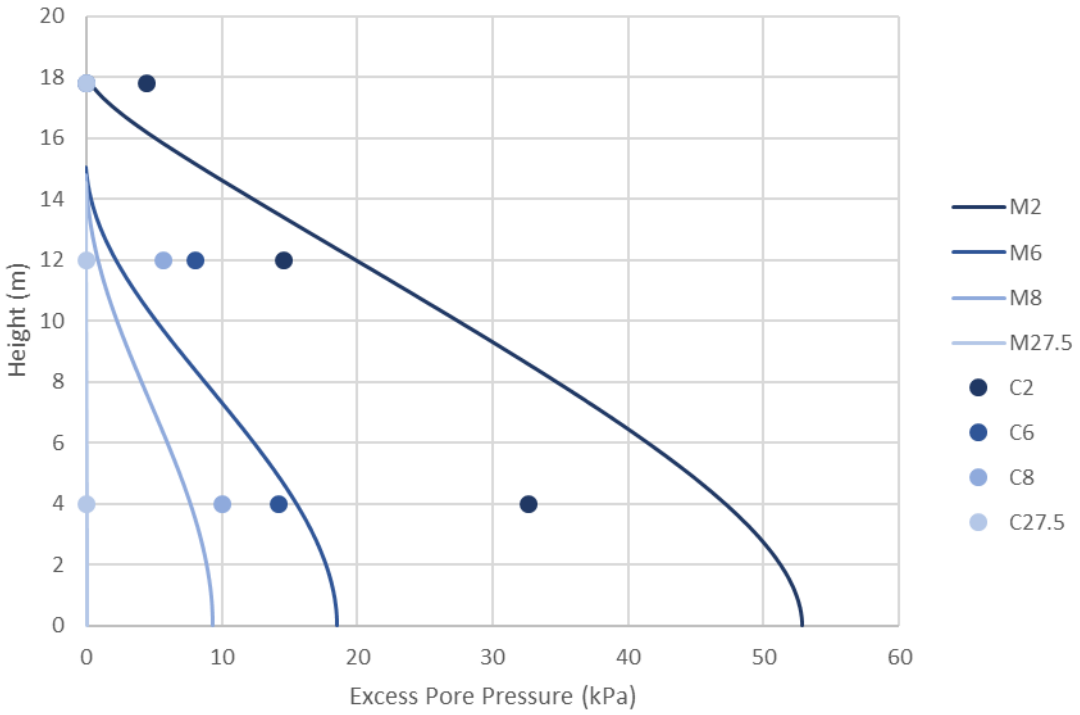

Figure 50 - Excess Pore Pressure Dissipation in Centrifuge and Numerical Model (Kaolinite Single Fill)

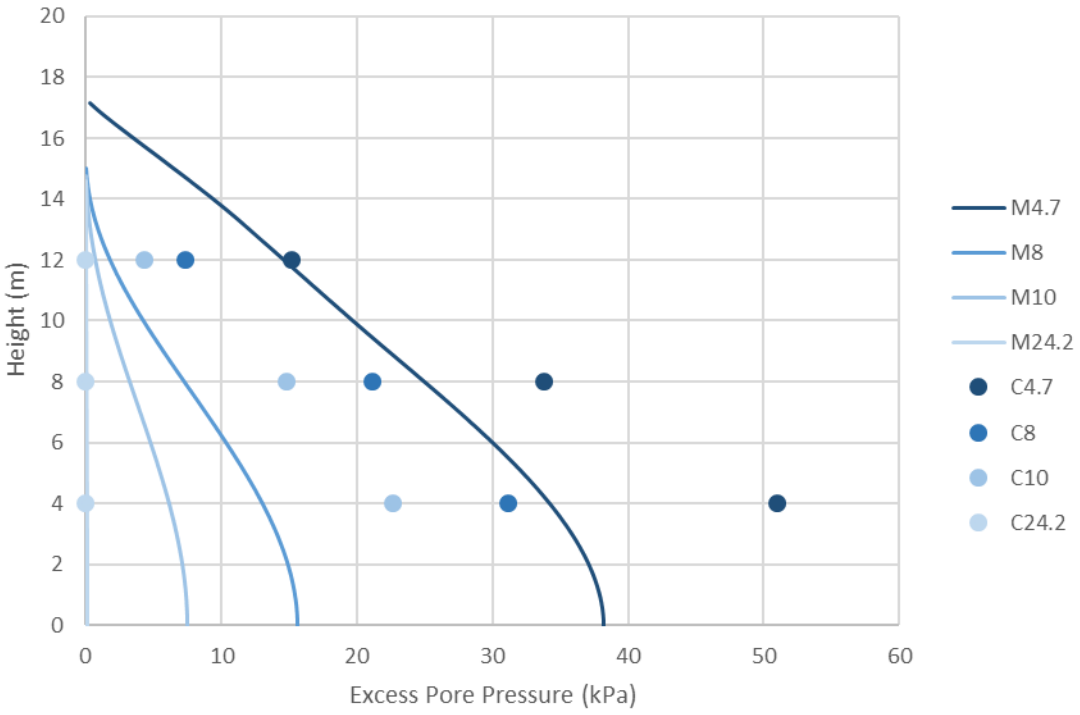

Figure 51 - Excess PP Dissipation in Centrifuge and Numerical Model (Kaolinite Layer Fill)

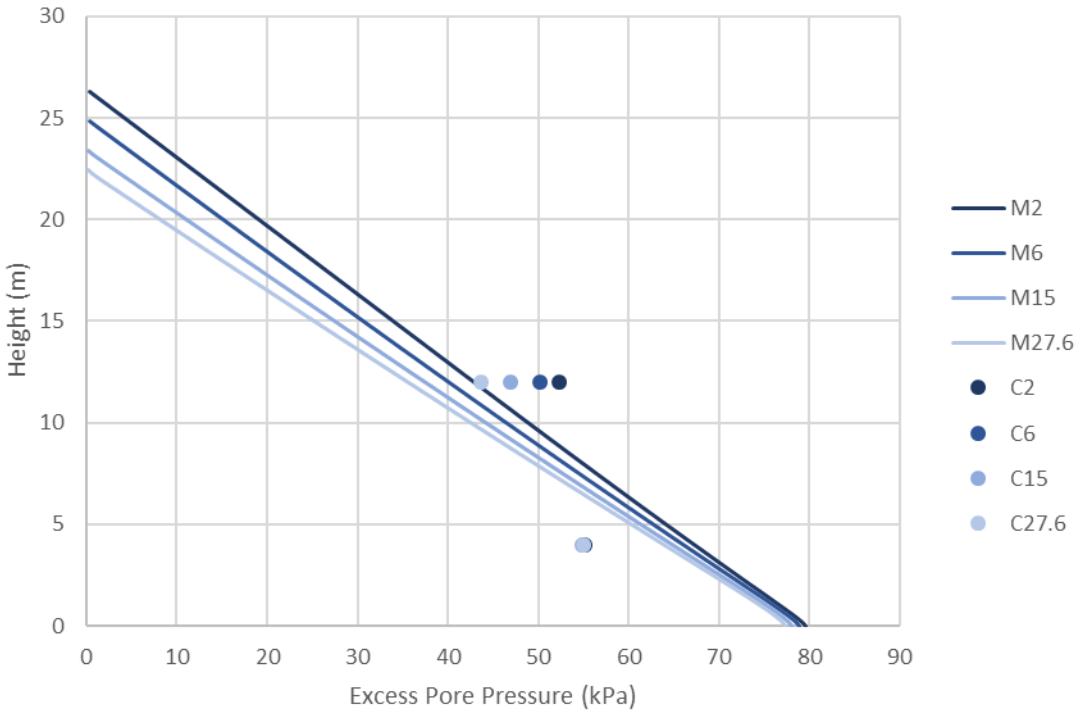

Figure 52 - Excess PP Dissipation in Centrifuge and Numerical Model (FFT Single Fill)

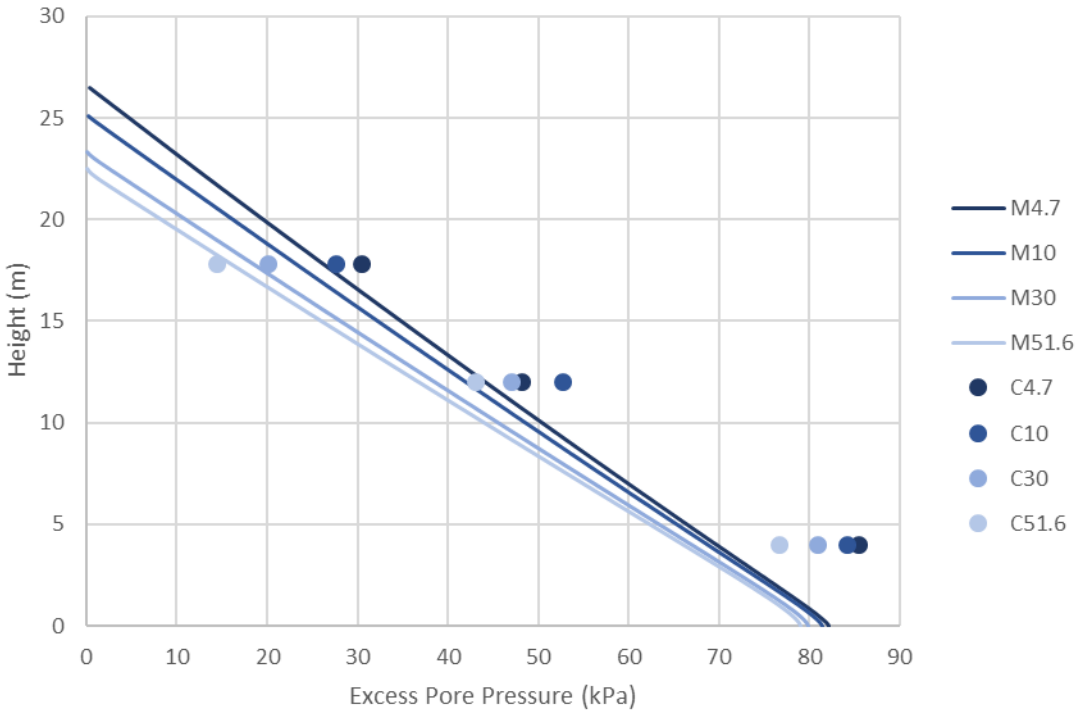

Figure 53 - Excess PP Dissipation in Centrifuge and Numerical Model (FFT Layer Fill)

5 Discussion

5.1 Settlement

In the kaolinite tests, the single fill model had an initial solids content of 39.0% and settled 13.5cm (47.5%) after 27.6 years of prototype time in the centrifuge. The layered kaolinite model, with an initial solids content of 38.4%, settled 14.6cm (50.2%) after 24.2 years of prototype time. For both the kaolinite single and layered fill schemes, ultimate settlement was achieved after approximately ten years of prototype time in the centrifuge. In the layered kaolinite tests, a significant amount of settlement was observed as each layer was loaded and allowed to settle in the centrifuge. Kaolinite was added in 4.6-5.2cm (average 4.85cm) layers to the consolidation cell (refer to Table 5), and the layers settled between 2.0-2.3cm (average 2.22cm) during the 1-hour of centrifuge consolidation between addition of new layers. The layered fill scheme achieved 2.7% more overall settlement than the single fill scheme in the kaolinite tests.

In the FFT tests, the single fill model had an initial solids content of 42.6% and settled 4.7cm (17.2%) after 27.6 years of prototype time in the centrifuge. The layered FFT model, with an initial solids content of 42.3%, settled 5.8cm (20.1%) after 24.5 years of prototype time, and 7.9cm (27.4%) after 51.4 years of prototype time. It is unknown how long it would take to achieve ultimate settlement of this material, as tests were terminated after 48 hours on the centrifuge. As demonstrated by Figure 29, the FFT model was still undergoing self-weight consolidation when the tests were terminated. FFT was added in 4.3-5.5cm layers (average 4.8cm) and settled 0.4-0.7cm (average 0.54cm) during the 1-hour of centrifuge consolidation between addition of new layers. In the FFT models, the layered fill model achieved 2.9% greater settlement than the single fill model after a similar prototype consolidation time.

There are several contributing factors that could have caused additional settlement in the layered versus single fill models:

- Different initial solids contents in layered versus single fill models
- Centrifuge spin time for layered versus single fill models
- Differences in stress between layered versus single fill models
- Higher effective G-level in layered versus single fill models

As stated previously, the initial solids content for the kaolinite tests was 39.0% and 38.4% for the single and layered models, respectively. In the FFT tests, the initial solids content was 42.6% and 42.3% for the single and layered models, respectively. This difference was small (0.6% for kaolinite and 0.3% for FFT)

and may be a result of lab sampling error of solids content. However, it may still have contributed to the difference in settlement between the layered and single fill models, as we expect greater settlement to occur in the same material with a lower solids content over a set time.

Centrifuge spin time is a possible factor for the discrepancy between single and layered model settlement. However, greater settlement was achieved in the layered kaolinite test after 24.2 years versus 27.6 years in the single fill test. The same observation can be made for the FFT tests: greater settlement was achieved in the layered fill model after 24.5 years than 27.6 years in the single fill model. Therefore, the layered models achieved greater settlement with less centrifuge consolidation time as compared to the single fill models.

Differences in stress between the single fill and layered models may have also contributed to the different settlement values. During the layered tests, water was decanted from the surface as each layer was added to the centrifuge consolidation cells; the cap water in the single fill tests was not decanted. Theoretically, the effective stress profiles would be consistent regardless of the decanted cap water. The stress profiles in the kaolinite models and FFT models at the end of testing are shown in Figure 54 and Figure 55, respectively (effective stress data was not available for the FFT models). In Figure 53 and Figure 54, data labelled “K-S Total” refers to the total stress profile at end of testing in the Kaolinite Single fill test; “K-L PP” refers to the final pore pressure profile at the end of testing in the Kaolinite Layered fill test.

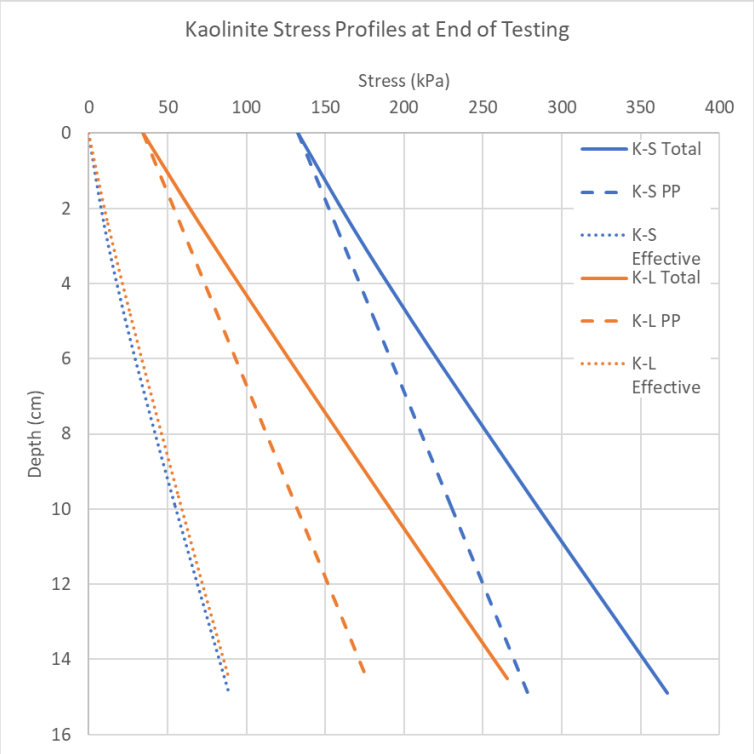

Figure 54 - Kaolinite Stress Profiles at End of Testing

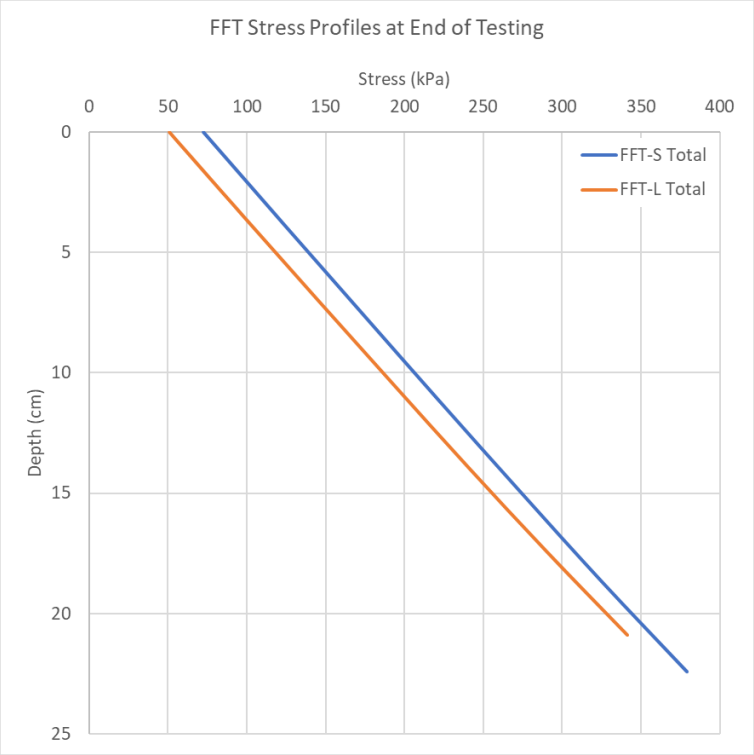

Figure 55 - FFT Stress Profiles at End of Testing

As demonstrated by the above figures, the layered kaolinite model appeared to have slightly higher levels of effective stress at the end of testing, compared to the single fill model. This slight increase in effective stress generated in the layered model may have attributed to the minor increase (2.7%) in settlement observed during testing. Effective stress profiles were not able to be generated for the FFT models, so it is unknown if a similar increase in effective stress was present in the layered FFT model.

Another consideration for the additional settlement in the layered models is the change in G-level with model height in the centrifuge. G-level is not constant throughout the entire depth of the model; it increases as the centrifuge radius increases (Figure 56). For the centrifuge used in this study, the calculation of G-level is given by Equation [5] :

$$G = \frac{rN^2}{895} \qquad [5]$$

Where *G* is the G-level in the centrifuge, *r* is the centrifuge radius, and *N* is the rotational speed of the centrifuge, in revolutions per minute (rpm). As previously discussed in Chapter 2, the G-level is often calculated at one-third the depth of the model to minimize error. However, small variations in the G-level still exist when following these guidelines.

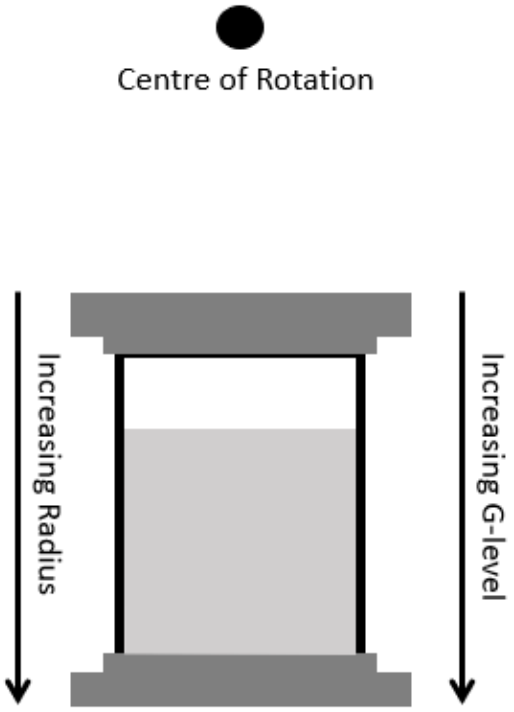

Figure 56 - G-level in Centrifuge Model

The average G-level within the centrifuge model can be found with the following expression:

$$G_{avg} = \frac{\int_{r_{top}}^{r_{bottom}} \frac{rN^2}{895} dr}{r_{bottom} - r_{top}} \quad [6]$$

Where r_{bottom} is the centrifuge radius at the bottom of the consolidation cell and r_{top} is the centrifuge radius at the top of the model interface. The results from this calculation are shown below in Table 10. KAL-S refers to the kaolinite single fill test, KAL-L refers to the kaolinite layered test, FFT-S refers to the FFT single fill test, FFT-L refers to the FFT layered test.

Table 10 - G-level Calculations for Centrifuge Models

	Max Initial Height (cm)	**Radius at Top**	**Radius at Bottom**	**G-level at Top**	**G-level at Bottom**	**G-level Average**
KAL-S	28.4	1.65	1.93	95.0	111	103
KAL-L	18.0*	1.75	1.93	101	111	106
FFT-S	27.3	1.66	1.93	95.6	111	104
FFT-L	26.1*	1.67	1.93	96.3	111	104

*The max initial height was taken as the interface height after all layers had been added to the model

As shown by the above calculations, the average G-level in the layered kaolinite model was slightly higher than that in the single fill kaolinite model. This is a result of the decreased height in the layered model. It is likely that this increased average G-level contributed to the increased settlement observed in the kaolinite layered model versus the single fill model. However, in the FFT models, the average G-level was consistent between the layered and single fill models, although increased settlement occurred in the layered model. Fox et al. (2005) examined impact of G-level variation within a soil specimen during centrifuge testing. It was found that for samples with a height ratio (sample height divided by centrifuge radius) of 0.2 or less, the computed settlement curves which accounted for G-level variability closely matched the results from the centrifuge tests which assumed a constant G-level. The height ratio used in the tests conducted in this thesis was 0.14 or less, meaning any discrepancy caused by variability of G-level within the centrifuge models should be small.

5.2 Void ratio profiles

When comparing the final void ratio profiles for the kaolinite centrifuge tests, it is observed that the layered fill kaolinite test had a lower void ratio in the uppermost sample points at end of testing as compared to the single fill test. In the lower sample points, the void ratio of the layered and single fill tests was similar. These results suggest that the additional consolidation observed in the layered versus single fill kaolinite tests had occurred in the uppermost layers, and consolidation in the lower layers was complete.

When comparing the final void ratio profiles for FFT centrifuge tests, it is observed that the layered fill FFT test had a lower overall void ratio as compared to the single fill test. There was no obvious difference observed at certain sample points like in the kaolinite tests. The final void ratio profile of the single and layered FFT tests had a similar shape at end of testing, though the layered FFT tests had lower overall void ratio due to longer spin time (48 hours in the layered test versus 24 hours in the single fill test).

5.3 Pore pressure response

In the kaolinite single and layered fill tests, the pore pressure response was observed to follow the expected profile: rapid dissipation at the start of consolidation and asymptotically approaching the hydrostatic value as consolidation continued. In the layered fill test, pore pressure dissipation is observed as each layer is added to the cell and allowed to consolidate. This is an expected response as material was being added to the consolidation cell.

In the FFT single fill test, it was observed that little pore pressure dissipation had occurred during testing; however significant interface settlement was observed (Figure 57). These results suggest that for this particular FFT material, there may be other driving forces behind the settlement beyond primary consolidation, as little to no effective stress had developed over the course of testing. A similar observation was made by another researcher.

Jeeravipoolvarn (2005) studied a series of large-scale standpipes at the University of Alberta. The standpipes were 10 m in height and filled with mature fine tailings mixtures of different sands-fines ratio. One such column (referred to as Standpipe 1 in the study) was measured as 89% fines content and is most similar to the tailings material used in this thesis. The standpipe was continuously monitored and sampled for pore pressures, solids content and density measurements. The interface settlement and stress profiles of this column were also continuously measured. It was observed that after 21 years of

monitoring, the tailings in this standpipe settled approximately 3 m with approximately zero effective stress developing (Jeeravipoolvarn 2005). Jeeravipoolvarn (2005) states that the settlement observed in this standpipe test is due to creep and not consolidation since zero effective stress was observed.

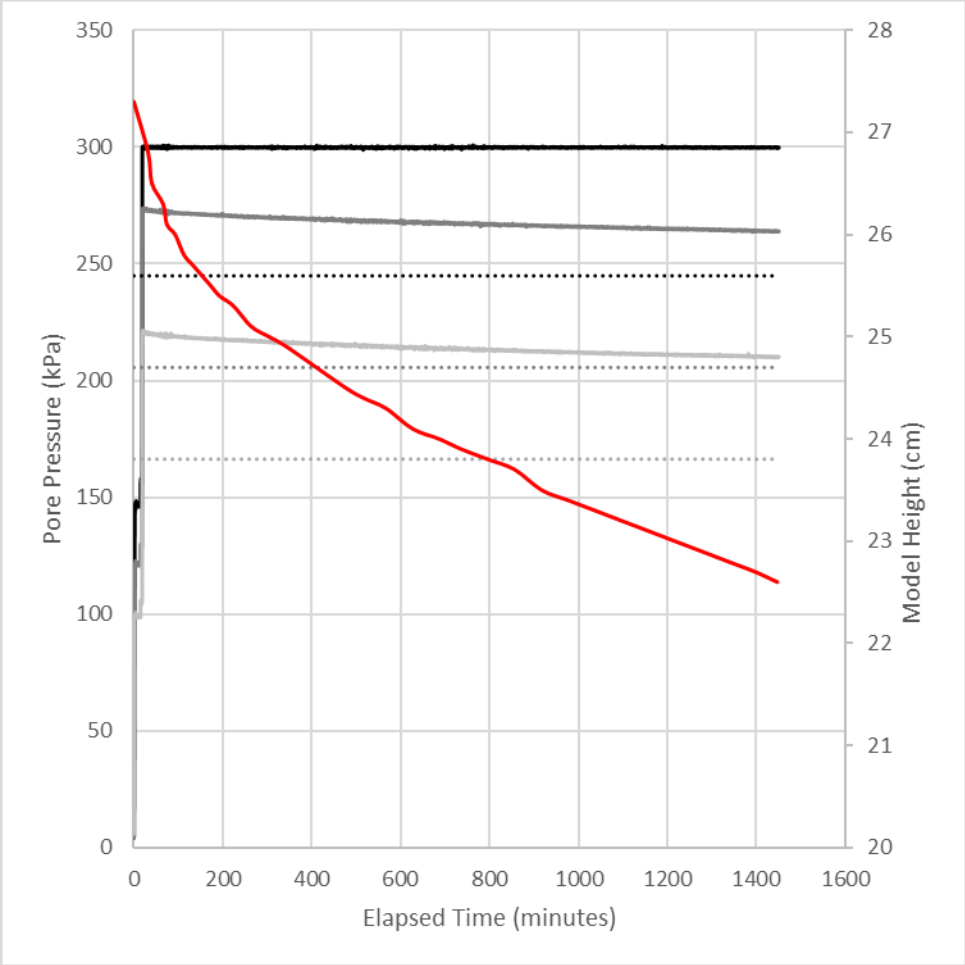

Figure 57 - FFT Single Fill Pore Pressure Dissipation and Interface Settlement

5.4 Comparison with numerical models

5.4.1 Settlement Curves

The settlement curves obtained from the numerical model were compared to the results obtained from numerical modelling software (FSCA). It was observed that ultimate settlement values were similar for both kaolinite and FFT tests, however the ultimate interface settlement was achieved in shorter time in the centrifuge tests versus the numerical model for both material types (Figure 44, Figure 45, Figure 47, Figure 48). To obtain a match between centrifuge and numerical model results, the permeability functions of the kaolinite and FFT were adjusted. A similar observation was made by (Sorta et al. 2016), and the author used adjusted permeability curves to obtain a closer match between model and

centrifuge. The author did not adjust the compressibility input parameters to obtain a match, only the permeability input parameters required adjustment. This is because the rate of settlement is controlled by the permeability function, whereas the compressibility function only controls the ultimate settlement (Jeeravipoolvarn 2005).

The original and adjusted input parameters used for the numerical modelling portion of this thesis are shown below in Table 11. In the kaolinite tests, the permeability parameter C=6.0x10^{-5} m/day was adjusted to C=3.0x10^{-4} m/day (a factor of 5). In the FFT tests, the permeability parameter C=5.0x10^{-10} m/day was adjusted to C=7.0x10^{-9} (a factor of 14). The adjusted values were chosen to provide the closest match to final interface height at end of testing.

Table 11 - Adjusted Permeability Functions for Numerical Model Inputs

Material	**A (kPa)**	**B (no units)**	**C (m/day)**	**D (no units)**
Kaolinite	3.956	-0.261	6.000x10^{-5}	3.756
Kaolinite (Adjusted k-curve)	3.956	-0.261	3.000x10^{-4}	3.756
FFT	2.514	-0.237	5.000x10^{-10}	12.131
FFT (Adjusted k-curve)	2.514	-0.237	7.000x10^{-9}	12.131

5.4.2 Void Ratio Profiles

When using the adjusted permeability function, the final void ratio profiles were closely matched between the centrifuge and numerical model for kaolinite (Figure 46). This result was expected due to the close match observed between the centrifuge and numerical model settlement profiles (using the adjusted permeability function).

Although interface settlement was equal at the end of testing, the void ratio profiles for centrifuge and numerical model tests was not in as close agreement for FFT as it was for kaolinite. Overall, the void ratio for FFT in the centrifuge was lower at all sample points compared to the numerical model (Figure 49).

5.4.3 Pore Pressure Profiles

In both the single and layer fill kaolinite tests, it was observed that the numerical model had lower excess pore pressure at the same chosen model heights and elapsed time when compared to results obtained from the centrifuge (Figure 50, Figure 51). These results are unexpected due to the close match between the centrifuge and numerical model settlement curves.

The excess pore pressure profiles obtained for the FFT were in agreement for the centrifuge tests and numerical model (Figure 52, Figure 53). As discussed previously, the excess pore pressures did not significantly dissipate during the centrifuge or numerical model tests due to the low hydraulic conductivity of the FFT material.

5.4.4 Discrepancy Between Centrifuge and Numerical Model Results

As discussed in section 5.4.1, the hydraulic conductivity of both the kaolinite and tailings materials was adjusted to match the settlement curves obtained with the numerical model and centrifuge results. It was observed that the settlement rate for both material types was higher in the centrifuge tests. However, the amount by which the hydraulic conductivity function was adjusted was unique for each material. For kaolinite, the C factor was increased by a factor of 5 and for the tailings it was adjusted by a factor of 14 (Table 11). This suggests that the hydraulic conductivity of the materials used in this study was higher in the centrifuge versus the LSCT tests which were originally used to determine the large strain consolidation relationships. A similar observation was made by (Sorta et al. 2016), who adjusted the hydraulic conductivity function to achieve a match between model and centrifuge results for several different test materials.

Sorta et al. (2016) determined the hydraulic conductivity function at different stages of consolidation for various materials using the centrifuge modelling technique and found that hydraulic conductivity in the centrifuge was generally higher than in the LSCT tests. It is not clear whether the hydraulic conductivity is consistently higher in the centrifuge by the same factor as compared to the LSCT tests, or if the value is unique for each material. Based on the results from this study, the value appears to be unique depending on the material type.

Sorta et al. (2016) also analyzed the compressibility functions of various materials during centrifuge consolidation and observed that compressibility of all materials was higher during the initial stages of consolidation compared to the LSCT compressibility. However, at the end of testing the centrifuge derived compressibility functions converged to the LSCT compressibility. Sorta et al. (2016) attributed to

this non-uniform compressibility to the strain rate: higher strain rates observed at the initial stages of consolidation led to greater compressibility. Towards the end of the centrifuge tests, observed strain rate decreased towards that of the LSCT, and compressibility functions converged.

Jeeravipoolvarn et al. (2008) examined the effect of varying the compressibility and hydraulic conductivity functions to history match the consolidation behaviour of a 10 m fine tailings filled column with a numerical model. The author used two approaches: the compressibility approach and the hydraulic conductivity approach. In the compressibility approach, the pre-consolidation and creep compression effects were accounted for in the model. In the hydraulic conductivity approach, the hydraulic conductivity was varied with depth, as it was theorized that hydraulic conductivity is lowest at the bottom of the model and is highest at the top of the model. For the compressibility approaches, it was found that these did not provide good agreement with the experimental data. For the hydraulic conductivity approach, there was good agreement between the model and experimental data, including interface settlement, void ratio measurements and effective stress predictions.

6 Conclusions and Recommendations for Future Work

6.1 Conclusions

The objective of this research was to develop and test a new centrifuge modelling method where slurry/tailings material is added continuously during testing. This new test method involved addition of material in six different layers, with consolidation of each layer occurring between each new layer addition. The layered fill test was completed on both a kaolinite slurry and a treated oil sands FFT material. Single fill tests were completed on the same materials and the resulted from both tests were compared. The centrifuge tests were also recreated using a large strain consolidation numerical model and the results were compared. Based on the test results, the following conclusions were made:

- A modelling technique using a layered addition of material was tested and used to model the consolidation behaviour of a kaolinite slurry and oil sands FFT in a geotechnical centrifuge.
- For both kaolinite and FFT, the layered tests achieved greater settlement for similar consolidation times, though this value was small for both materials (<3%). This additional settlement was attributed to minor differences in initial solids content for both materials, and variations in G-level within the models during testing.

- Significant settlement was observed in the FFT single and layered fill tests without developing significant effective stress. This result suggests other driving forces are responsible for the settlement observed in this material besides primary consolidation.
- Compression and hydraulic conductivity functions were derived from both centrifuge and LSCT tests for use in a large strain consolidation numerical model. It was observed that for both kaolinite and FFT, the single and layered centrifuge tests had higher settlement rates versus the numerical model, but similar ultimate settlement. Centrifuge and numerical model results agreed when using adjusted hydraulic conductivity functions. The magnitude the hydraulic conductivity functions were adjusted was unique for both kaolinite and FFT. The magnitude of this adjustment appears to be unique for each material and not a constant for centrifuge modelling.

6.2 Recommendations for Future Work

Several new questions arose during the research conducted as part of this thesis. The following are potential areas of new research:

- Develop a method to monitor the individual interface between each layer in the centrifuge consolidation cell. This will provide additional insight into the consolidation behaviour in the layered fill models.
- Further research is needed to understand the consolidation behaviour of the FFT material (and similar oil sands tailings materials) used in this thesis. Based on the results from this research, primary consolidation may not be the driving force of the settlement observed in the FFT.
- Further research is needed to understand the variability of hydraulic conductivity within the centrifuge consolidation models. Based on the results, hydraulic conductivity functions derived from LSCT tests were adjusted in the numerical model to achieve agreement with centrifuge results. The magnitude of this adjustment was unique for each material.

References

AER. 2019. State of fluid tailings management for mineable oil sands, 2018. .

AER. 2018. Alberta's energy reserves and supply/demand outlook . ST98, Alberta Energy Regulator, Calgary, Alberta.

AER. 2016. Mineable oil sands fluid tailings status report 2014 and 2015. Alberta Energy Regulator, Calgary, Alberta.

Antonaki, N., Abdoun, T., and Sasanakul, I. 2017. Consolidation and dynamic response of a layered mine tailings deposit in centrifuge tests, Geotechnical Testing Journal, **40**(5): 746-761.

ASTM International. 2017. *ASTM D7928-17 standard test method for particle-size distribution (gradation) of fine-grained soils using the sedimentation (hydrometer) analysis*. .

BGC Engineering Inc. 2010. Oil sands tailings technology review. OSRIN Report No. TR-1, Oil Sands Research and Information Network, niversity of Alberta, School of Energy and the Environment, Edmonton, Alberta.

Cargill, K.W. and Ko, H. 1983. Centrifugal modelling of transient water flow, Journal of Geotechnical Engineering, **109**(4): 536-555.

Chalaturnyk, R., J., Scott, J., D., and Ozum, B. 2002. Management of oil sands tailings, Petroleum Science and Technology, **20**(9 & 10): 1025-1046.

COSIA. 2018. Tailings reduction technology [online]. Available from https://www.cosia.ca/initiatives/tailings/projects/tailings-reduction-technology [cited November 9 2018].

Dunmola, A., Wang, N., Lorentz, J., Chalaturnyk, R., Zombrano, G., and Song, J. 2018. Comparison of geotechnical beam centrifuge predictions to field data from 10m deep FFT centrifuge cake columns. *In* International Oil Sands Tailings Conference, Edmonton, Canada.

Eckert, W., F., Masliyah, J., H., and Gray, M., R. 1996. Prediction of sedimentation and consolidation of fine tails, American Institute of Chemical Engineers Journal, **42**(4): 960-972.

Fisseha, B., Wilson, G., and Simms, P. 2018. Assessment of self-weight consolidation of flocculated fluid fine tailings under various environmental conditions. *In* Proceedings of the 21st International Seminar on Paste and Thickened Tailings, Perth, pp. 291-304.

Flach, P.D. 1984. Oil sands geology - athabasca deposit north. Geological Survey Department, Alberta Research Council, Edmonton, Alberta, Canada.

Fox, P.J., Lee, J., and Qiu, T. 2005. Model for large strain consolidation by centrifuge, International Journal of Geomechanics, **5**(4): 267-275.

Gibson, R.E., England, G.L., and Hussey, M.J.L. 1967. The theory of one-dimensional consolidation of saturated clays, Geotechnique, **17**: 261-273.

Government of Alberta. 2018. About oil sands: Facts and statistics [online]. Available from https://www.energy.alberta.ca/OS/AOS/Pages/FAS.aspx [cited November 05 2018].

Jeeravipoolvarn, S. 2010. Geotechnical behaviour of in-line thickened oil sands tailings. PhD, University of Alberta, Edmonton, Alberta, Canada.

Jeeravipoolvarn, S. 2005. Compression behaviour of thixotropic oil sands tailings. Master, University of Alberta, Edmonton, Alberta, Canada.

Jeeravipoolvarn, S., Chalaturnyk, R., J., and Scott, J., D. 2008. Consolidation modeling of oil sands fine tailings: History matching. *In* GeoEdmonton 2008, Edmonton, Alberta, pp. 190-197.

Kabwe, K.K., Scott, J.D., Wilson, G.W., and Sorta, A. 2014. From fluid to solid: Oil sands fluid fine tailings. *In* 7th International Congress on Environmental Geotechnics, Melbourne, Australia.

Kasperski, K.L. and Mikula, R.J. 2011. Waste streams of mined oil sands: Characteristics and remediation, Elements, **7**(6): 387-392.

Kayabali, K. and Ozdemir, A. 2012. Assessing the practicality of the centrifuge method for 1-D consolidation, Bulletin of Engineering Geology and the Environment, **71**: 735-745.

Klark, K.A. and Pasternack, D.S. 1949. The role of very fine mineral matter in the hot water separation process as applied to athabaska bituminous sand. 53, Research Council of Alberta, Edmonton, Alberta, Canada.

Ko, H. 1988. Summary of the state of the art in centrifuge model testing. *In* Centrifuge in Soil Mechanics *Edited by* Craig WH, James RG, Schofield AN. , pp. 11-28.

McKenna, G., Mooder, B., Burton, B., and Jamieson, A. 2016. Shear strength and density of oil sands fine tailings for reclamation to a boreal forest landscape. *In* 5th International Oil Sands Tailings Conference, Lake Louise, Alberta, Canada.

Mizani, S., He, X., and Simms, P. 2013. Application of lubrication theory to modeling stack geometry of high density mine tailings, Journal of Non-Newtonian Fluid Mechanics, **198**: 59–70.

Mossop, G.D. 1980. Geology of the athabasca oil sands, Science, **207**(4427): 145-152.

NEB. 2000. Canada's oil sands: A supply and market outlook to 2015. Energy Market Assessment, National Energy Board, Ottawa, Canada.

Nik, R., M. 2013. Application of dewatering technologies in production of robust non-segregating tailings. PhD, University of Alberta, Edmonton, Alberta, Canada.

OSTC. 2012. Technical guide for fluid tailings management. Oil Sands Tailings Consotrium, Calgary, Alberta.

Reid, D. and Fourie, A., B. 2012. Accelerated consolidation of soft clays and mine tailings using a desktop centrifuge. *In* 16th International Conference on Tailings and Mine Waste, Keystone, Colorado, USA, pp. 17-28.

Roscoe, K.H. 1968. Soils and model tests, Journal of Strain Analysis, **3**(1): 57-64.

Scott, J.D., Jeeravipoolvarn, S., and Chalaturnyk, R., J. 2008. Tests for wide range of compressibility and hydraulic conductivity of flocculated tailings. *In* 61st Canada Geotechnical Conference, Edmonton, Alberta, pp. 738-745.

Singh, D., N and Gupta, A., K. 2000. Modelling hydraulic conductivity in a small centrifuge, Canadian Geotechnical Journal, **37**(5): 1150-1155.

Sobkowicz, J.C. and Morgenstern, N.R. 2009. A geotechnical perspective on oil sands tailings. *In* Tailings and Mine Waste 2009, Banff, Alberta, pp. xvii-xxix.

Sorta, A., R. 2015. Centrifugal modelling of oil sands tailings consolidation. PhD, .

Sorta, A., R., Sego, D., C., and Wilson, W. 2016. Physical modelling of oil sands tailings consolidation, International Journal of Physical Modelling in Geotechnics, **16**(2): 47-64.

Sorta, A., R., Sego, D., C., and Wilson, W. 2012. Effect of thixotropy and segregation on centrifuge modelling, International Journal of Physical Modelling in Geotechnics, **12**(4): 143-161.

Stone, K., Randolph, M., Toh, S., and Sales, A. 1994. Evaluation of consolidation behaviour of mine tailings, Journal of Geotechnical Engineering, **120**(3): 473-490.

Takada, N. and Mikasa, M. 1986. Determination of consolidation parameters by selfweight consolidation test in centrifuge. *In* Consolidation of Soils: Testing and Evaluation, ASTM STP 892 *Edited by* R. Yong and F. Townsend. American Society for Testing and Materials, Philadelphia, pp. 548-566.

Taylor, R., N. 1995. Geotechnical centrifuge technology. Blackie Academic & Professional, London.

TBS. 2012. Operating manual for GT50/1.7 geotechnical beam centrifuge. Thomas Broadbent & Sons, Ltd., UK.

Townsend, F., C., Bloomquist, D., G., McClimans, S., A., and McVay, M., C. 1986. Volume 1: Centrifugal model evaluation of reclamation schemes for phosphatic waste clay ponds. *In* Reclamation of Phosphatic Clay Waste Ponds by Capping *Edited by*Florida Institute of Phosphate Research, Bartow, Florida.

Zambrano-Narveaz, G. and Chalaturnyk, R., J. 2014. The new GeoREF geotechnical beam centrifuge at the university of alberta, canada. *In* , Vol. Proceedings of the 8th International Conference on Physical Modelling in Geotechnics, pp. 163-167.

Znidarcic, D., Miller, R., van Zyl, D., Fredlund, M., and Wells, S. 2011. Consolidation testing of oil sand fine tailings. *In* Proceedings Tailings and Mine Waste, Vancouver, BC.